4.1 Spontaneous resolution through supramolecular self-assembly:

Non-covalent π–π interaction is one of the key elements in the self-assembly of organic molecules.[1] this is one of the very important phenomena which have direct or indirect impact on all the streams of science. One of the illustrative examples showing their importance is the double helix of the DNA; not only stabilized by hydrogen bonding but also by other electrostatic forces between the stacked base pairs. If somehow we remove these electrostatic forces, the important helical structure of the DNA double helix will collapse and it will not be able to store and transfer genetic information.[2] Effective control and understanding of chirality is very important in self-assembly procedures. It can, not only provide the answers to basic questions such as the of origin of chirality in biological systems, but also help us in design and synthesize molecules with better substrate-receptor relationship, more effective building blocks for supramolecular complexes with unique properties and also develop new means of chiral separations. Research that will explain the transfer of chirality over the long range is of high price in pharmaceutical and material science.

Homochiral or preferential crystallization is one of the simplest ways to separate racemic mixture. In 1848, Louis Pasteur, discovered the first, separation of enantiomers by homochiral crystallization of a conglomerate. Pasteur visually identified and physically separated these crystals based on their appearance. After separating the crystals into two enantiomorphous groups and dissolving them, he found that the two solutions rotate polarized light in opposite directions.[3] this rare and uncommon event was considered as milestone in chemistry of optically active molecules.[4] Enrichment of enantiomers of solids by crystallization from solutions with low optical purity has been known to occur in few cases.[5] Such examples are limited to certain type of crystal arrangement and polymorphism which allows deposition of nonracemic crystals under preferential enrichment conditions.[6]

Types of crystal packing in enantiomers:

When crystallization of a racemic compound is carried out, three common types of packing is usually observed.[7]

1. **Racemic Compound:** is the one in which both the enantiomers are present in equal ratio. Approximately 90–95% of all crystalline mixtures form racemic compounds.
2. **Conglomerate:** is in fact, a mechanical mixture of enantiomerically pure crystals of one enantiomer and its opposite. So overall sample will be racemic because it also

contains other enantiomer.[8] This is the case for approximately 5–10% of all chiral crystalline molecules.

3. **Solid solution or Pseudoracemic compounds** in which the crystal contain equal number of molecules of both the enantiomers but arrangement is random. Less than 1% of the cases a racemic mixture crystallizes as a solid solution.

Only the second category, conglomerate shows spontaneous resolution. ***The segregation of enantiomers upon crystallization is known as spontaneous resolution. This is based on a preference of a molecule to make contacts with neighbors of the same chirality sense through supramolecular interactions.***

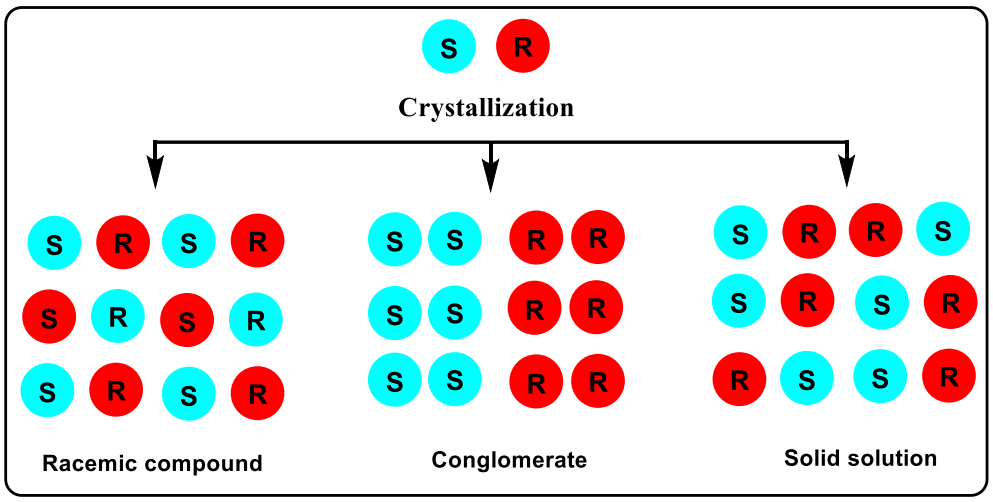

Figure 4.1: Types of crystal packing in molecules.

4.2 Designing molecules for spontaneous resolution:

Designing molecules which can spontaneously and selectively assemble in the desired stereochemistry require two important factors. First, to choose the most suitable functional groups which can promote the recognition through various non-covalent interactions such as hydrogen bonding, π-π interaction, Van derWaal's interaction, and can ultimately lead to self-assembly. Second and possibly more important as well as difficult part is to eliminate the undesired interactions which may weaken or nullify the effect of appropriate interactions. Crystallization is the most economical way to obtain enantiopure compounds, especially when the crystals can form conglomerate. However the possibility and predictability of conglomerate is a challenging task as only 5-10% of compounds show this behavior. Considerable progress is being made in the crystal prediction[9] but it is difficult to guarantee the predictability even with powerful analytical and computational techniques.

4.3 Detection of conglomerates:

How do we know that crystallized compound is a conglomerate? Starting from the racemic mixture it is often necessary to synthesize series of derivatives that have to be analyzed in order to isolate at least one conglomerate forming system, due to the low occurrence of conglomerates, it usually requires to scrutinize a large number of derivatives. Conglomerate detection which is an essential step of the resolution method can be pursued by various methods which are described and discussed in the following section. Immediate answer can be obtained by analyzing the single crystal structure of the compound. We need to check whether crystals fall in the category of chiral space group or not, If it shows chiral space group then there is possibility of conglomerate formation. But the observation of chiral space group is not conclusive as sometimes racemic molecules shows chiral space group because of crystal twinning or stacking of opposite enantiomers on the top of each other. Crystallographic parameters must be backed by other techniques such as optical rotation value, circular dichroism spectra (CD spectra) and HPLC to reach firm conclusion. Marked difference in the melting point of a racemate and its pure enantiomer is an indicator of a formation of conglomerate.

4.4 Spontaneous resolution of helical molecules:

In 1952 McIntosh[10] for the first time confirmed the structure of [5]helicenes by X-ray crystallographic, which showed the helical backbone due to the steric hindrance of the terminal rings. Thereafter interestingly Schmidt and Hahn reported crystal structures of helical molecules (**1** and **2**) crystallized in chiral space groups [11] however their chirality was not confirmed by any other supporting technique such as their optical rotation. Martin *et al.* [12] in 1968 reported the synthesis of [7]helicene **3** followed by the crystallization in benzene and the crystals were found to be optically active. Martin and coworkers beautifully designed the crystallization technique for resolution of helical molecules. Wynberg considered this as Martin's "crystal-picking technique". This optically active enantiomer of **3** was dextrorotatory with a high specific rotation value 6200 ($CHCl_3$). In continuation of his work; Martin extended this technique for resolution of [6], [7], [8] and [9]helicenes.[13] Although the technique was not successful in all the cases but this is indicative of strong interaction between the homochiral helicenes which allow optical resolution by crystal picking. Helical molecules not only

show spontaneous resolution but also form very interesting self-assemblies with unusual properties and applications. Spontaneous aggregation of optically active helicene bisquinone **4** was reported by Katz *et al* in 1996,[14] This compound assembled in to long fibrous aggregates with highly enhanced opto electronic properties such as high CD spectral intensity and exceptionally high optical rotation value. The enantiopure thiaheterohelicene **5** aggregated in a columnar fashion exhibiting good nonlinear optical properties.[15] helically twisted columnar discotic liquid crystals[16] **6** exhibited a novel type of self-assembly showing a hollow six stranded helical columns consisting a rare six repeat units with a perfect hexagonal structure.[17] Tanaka and co workers showed presence of hydrogen bonding functionalities help in the self assemblies of helical **7**.[18] Branda *et al.* showed a cooperatively self-assembly in a new helical molecule **8** consisting two binding sites at the terminal position of the framework.[19]

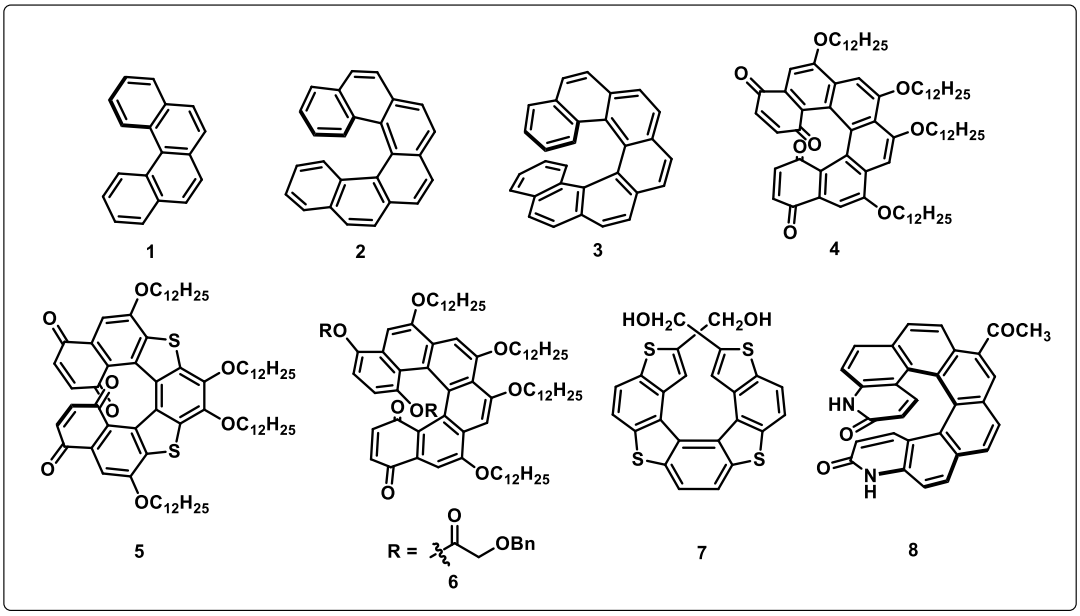

Figure 4.2: Helicene molecules with reported self-assembly behavior.

4.5 Spontaneous resolution of helicenes on surfaces:

This interesting phenomenon of chirality transfer and the long range expression in molecular self-assembly have been studied on various surfaces. These studies involve prochiral as well as chiral molecules. Understanding the fundamental forces that guide chiral molecular aggregations on surfaces is crucial to enabling the design of functional enantiospecific surfaces, organic transistors and bio sensors, thereby maximizing their potential. Some representative examples of such studies are outlined here. Ernst and co-workers first studied the self-assembly of [7]helicene **3** in 1999, and they found

formation of ordered monolayer of optically pure helicenes on Ni(111).[20] Taniguchi and co-workers [21] studied the self-assembly of thia[11]helicene **9** on gold surfaces and a 2D ordered layer was observed by STM and low-energy electron diffraction. The structures of the Au surface plays an important role in the understanding the behaviors of different types of assemblies formed. (*M*)-[7]helicene-2-carboxylic acid **10** self-assembles into island structures, while the racemate gives nanowire-like aggregates.[22] Parschau et al.studied the chirality transfer of [7]helicene **3** in the growth of 2D islands by van der Waals (vdW) interactions.[23] Seibel et al. described the 2D separation of pentahelicene **11** into homochiral domains purely through vdW forces.[24] Ivasenko *et al.* described the impact of chirality and the hydrogen bonds on the self-assembly of amino [7]helicene[25] **12.** They established that the presence of NH_2 group is essential for self-assembly on Au surface as it is oriented downward towards the surface. Ernst and co-workers discovered that the dispersive forces could act as polar forces in the metal surfaces. When racemic pentahelicene was deposited on the Cu(111), spontaneously resolution was observed in ordered regions, giving enantiomorphs composed by (*P*)- or (*M*)-enantiomer.[26] Several other examples of deposition of heptahelicene on Cu(111),[27] Cu (332), [28] Ni (100),[29] Ni (111),[30] and on SiO_2[31] are reported.

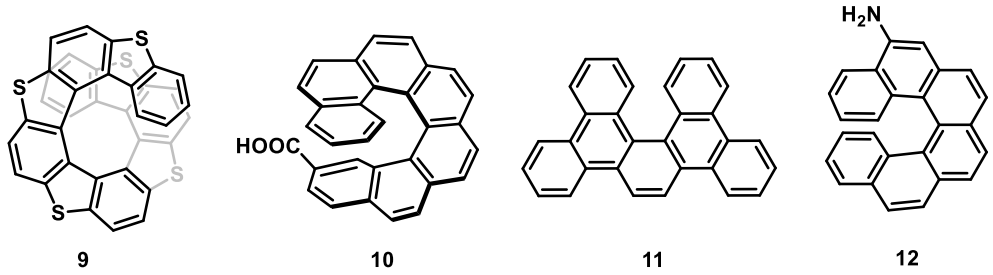

Figure 4.3: Reported helicenes showing self-assembly on various surfaces.

4.6 Cyano helicenes and conglomerate formation:

Literature citation suggests that very few synthons have the ability to show spontaneous resolution, and there is lack of correlation between the functionality and positions on the process of conglomerization. Wachsmann *et al* [32] while preparing the comparative data bank for hexahelicene observed that out of seven derivatives of hexahelicenes only the cyano hexahelicenes **13** showed conglomerate formation. Compound **13** on crystallization from benzene gave orange red crystals. Space group was found to be $P6_122$ indicating spontaneous resolution has happened. The detailed study of crystal structure reveals presence of well-defined intermolecular π-π interactions responsible for molecular recognition. Stöhr et al. [33] showed the spontaneous resolution of (±)-6,13-

dicyano[7]-helicene **14** is driven by polar interactions. They studied the self-assembly and 2D spontaneous resolution of cyano helicene on Cu(111) surface. This was the first example of the 2D spontaneous resolution, on Cu(111), of a racemic mixture of helicenes into long-range-ordered, fully segregated domains of pure enantiomers (2D conglomerate). This self association is based on supramolecular interactions such as CN···HC(Ar) hydrogen bonding and dipolar CN···CN interactions.

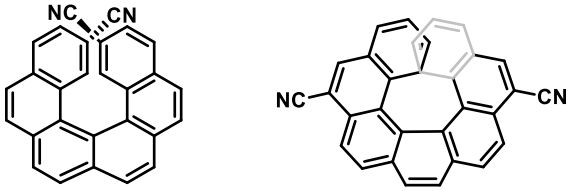

13 14

Figure 4.4: Reported cyano helicenes showing spontaneous resolution.

4.7 Results and Discussion:

4.7.1 Synthesis of cyano aza[7]helicenes:

Synthesis of title compound 5,13-dicyano-9-butyl-9*H*-aza[7]helicene **16** was achieved from 2,6-diformyl carbazole, via its bis-styryl type derivative **15** prepared by Knovenagel condensation with benzyl cyanide. Conversion of **15** to the target aza[7]helicene was easily done by photodehydrocyclization procedure involving a double, regioselective angular-angular cyclization to afford the compound **16** in good overall yield (**Scheme 4.1**). To establish the role of the *N*-attached side chain and the location of the cyano group and to study the effect of other substituent on the mode of molecular recognition and spontaneous resolution, we have designed a set of derivatives **17-20** (**Scheme 4.1 & 4.2**). The objective was to synthesize helicenes by introducing functional groups which may enhance the intramolecular CH−π interactions, dipolar interactions such as the presence of additional cyano group in **18**, a methoxy group in **17**, and a phenyl group in the side chain of **19** or by altering the positions of the cyano group **20**.

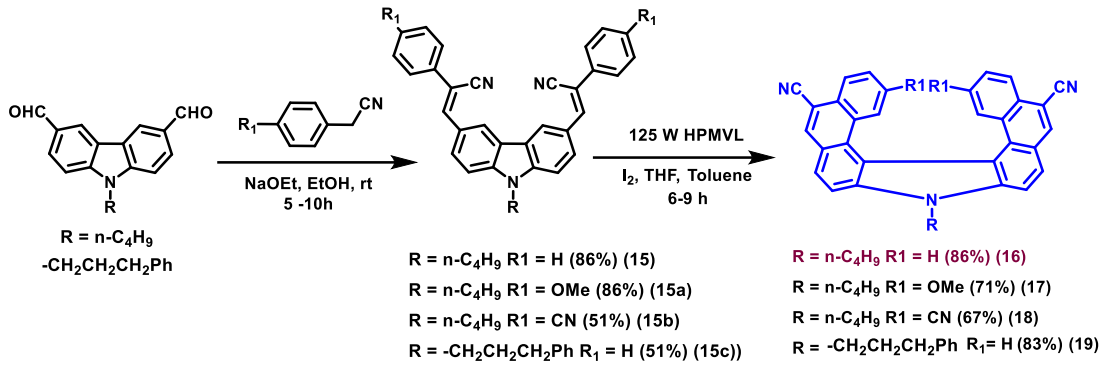

Scheme 4.1: Synthesis of cyano aza[7]helicenes.

Compound **20** was synthesized by different route where the diiodo carbazole was treated with *p*-cyano styrene under Heck reaction conditions to get bis styryl derivative **15d** followed by photocyclization.

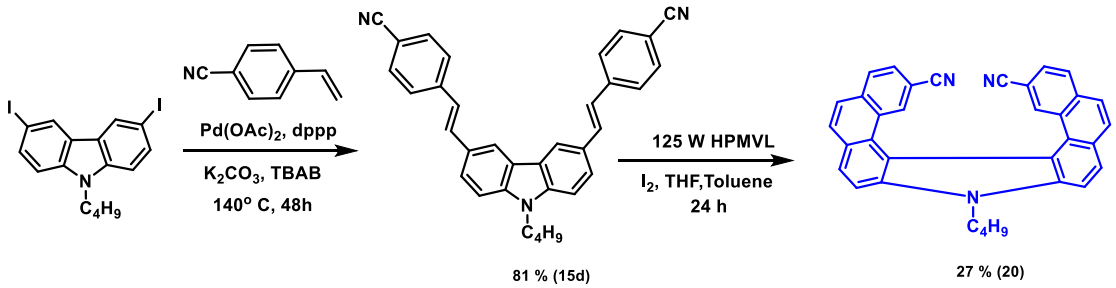

Scheme 4.2: Synthesis of compound **20**.

Total five derivatives of cyano aza[7]helicenes have been synthesized.

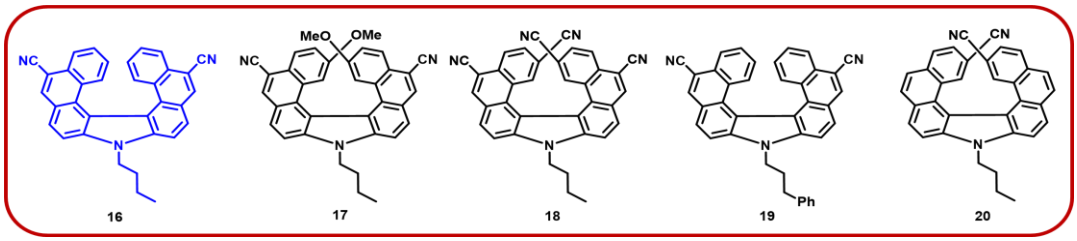

Figure 4.5: Synthesized Cyano aza[7]helicenes.

4.7.2 Crystal Structure, supramolecular superhelix and spontaneous resolution:

After the synthesis of desired target molecule **16**, we undertook the study of conglomerate formation by crystallizing **16** in different solvents. The initial attempts to enrich the helical enantiomers of **16** by crystallization in dichloromethane, toluene, hexane-chloroform, THF etc. resulted in the isolation of only racemic crystals. The plate like crystals of (±)-**16** were obtained from dichloromethane (**Figure 4.7**). This

sample crystallized into a monoclinic crystal system with centrosymmetric $P2_1/c$ space group containing both *P* and *M* isomers with the inclusion of dichloromethane. It was observed that compound (±)-**16** showed a non-planar herringbone-like packing pattern (along *b*-axis) by multiple C-H·····π interactions (3.214Å). Dichloromethane showed Cl···Cl bonding (3.135 Å) and hydrogen bonding with butyl chain of other isomer while its hydrogen showed bonding with cyano groups of same isomer along *a*-axis. Molecules of *P*/*M* description recognized the same isomer and formed 1D helical chain with opposite direction along *a*-axis. Hence, from crystal engineering point of view, one can predict that if solvent molecules do not get crystallized into crystal structure, the *P*/*M* isomers may get resolved into separate enantiomers i.e. conglomerates. To support the same, we studied effect of temperature on the same plate like crystal. On heating the crystal became opaque (60°C) while at higher temperature (100°C) it got disintegrated into smaller opaque crystals. The *n*-butyl chain of compound (±)-**16** remains orthogonal to helicene molecule and dihedral angle of helicene of both isomers is 82.51.°

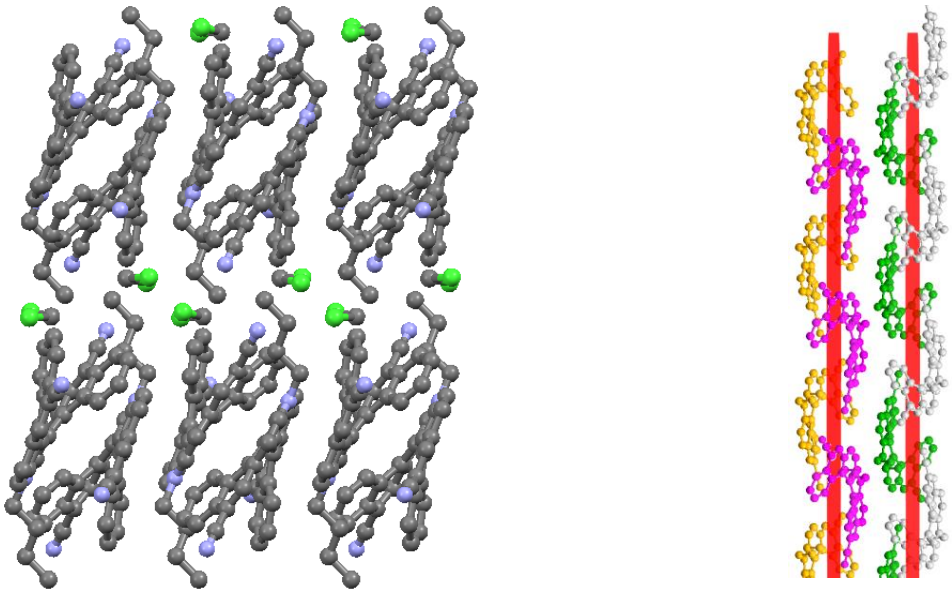

(a) **(b)**

Figure 4.6: (a) non-planar herringbone-like packing pattern along *b*-axis; (b) anti-parallel helical chains of P and M isomer along *a*-axis.

At the same time, crystallization from 1, 2-dichloroethane resulted in different type of crystals. These crystals were developed by slow evaporation of dilute solution of **16** in dichloroethane (0.2 g in 5 mL) resulting in a mixture of slightly dark, yellow colored uniformly diamond shaped transparent diffraction-quality crystals, along with some

twined crystals (**Figure 4.7**). The crystals were carefully handpicked and analyzed. The dark colored diamond shape ones were found to be either *P* or *M* in conformation which cannot be distinguished by color and crystal habit, while the twined ones were enriched with either isomer.

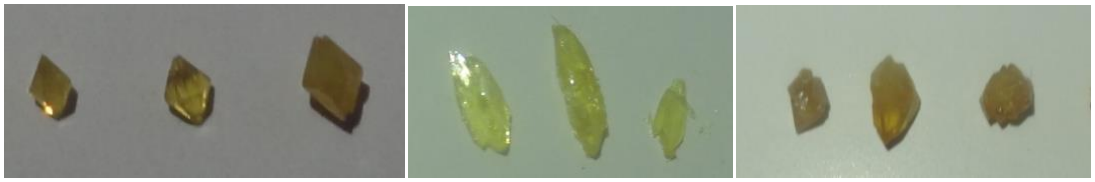

Figure 4.7: Optically pure diamond shaped (left) and racemic plate shaped (middle) and twinned (right) crystals of **16**.

The single crystal X-ray analysis of randomly picked diamond shaped crystal showed interesting molecular packing. Sample of (*P*)-**16** and (*M*)-**16** molecule crystallized into hexagonal crystal system with homochiral single-handed, enantiomerically-pure helicenes through self- assembly having chiral space group $P6_1$ and $P6_5$ respectively. A 6_1 axis corresponds to a right-handed helix; whereas 6_5 correspond to a left-handed helix (the two helices being enantiomorphous). The absolute configuration of enantiopure (*P*)-**16** was assigned on the sign of its observed optical rotation and confirmed by the refinement of the Flack parameter (0.08 with su 0.012). The absolute character of the crystal was further confirmed by SOR value and CD spectra. Literature survey shows that, such helicene structure with a perfect hexagonal symmetry has been rarely reported.[17] Spontaneous resolution gives (*P*)-**16** and (*M*)-**16** crystals by their conglomerate formation. It could be the result of the chiral recognition during crystallization in which the helicene molecule favored the helicene with same configuration. Initial rotation search identified the *c*-axis of the unit cell as the helical axis indicative of the formation of stable helical conformation. The crystal structure of enantiopure (*P*)-**16** and (*M*)-**16** was distinguishable from that of (±)-**16**, as enantiomer (*P*)-**16** forms a true hexagonal structure of right-handed helical columns (viewed from *c*-axis), unlike its enantiomer (*M*)-**16** with a left-handed helical column. The 1D channel can also be viewed as a composition of a number of cylindrical columns with *C*6 symmetry where each enantiomer shows three different helical motifs parallel to the c-axis, which in turn is made up of a rich array of molecular interactions (CH$\cdots\pi$ interactions and -CN$\cdots$H bonding). Seven molecules are present to complete one helical groove or motif in all helical columns around the 6_1 helical axes, where six units

(shown in six colors **Figure 4.9**) are arranged along with the central assembly (grey color). Such unexpected tight packing of helices show an infinite right hand helix structure (*P*) made up of exclusive units of the same handedness. The butyl chain which remains upward in the direction is not perpendicular to helicene as in case of (±)-**16**, where the terminal methyl bends in magic angle (106.88º). The butyl chain plays an important role in forming such super helix assembly of conglomerate resulting in enrichment of each isomer.

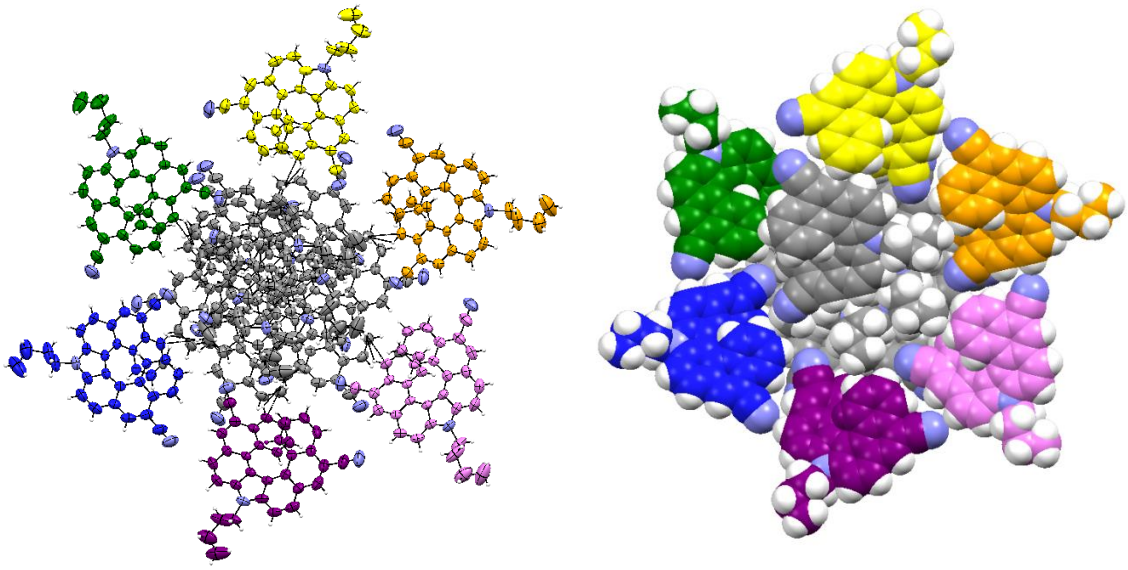

a b

Figure 4.8: (a) Super-helix arrangement involving CN···H interactions helical column along 6_1 screw axis at *c*-axis (b) CH---π interaction helical column along 6_1 screw axis at *c*-axis.

It is very important to understand the interactions responsible to form such self-assembly and spontaneous resolution. It is important to know the nature of contacts between molecules which crystallize out in optically pure form from racemic mixture to understand the mechanism of conglomerate formation. The closer look at crystal structure reveals three major interactions took place in the crystal structure of compound **16**. First helical assembly formed by -CN·····H interactions connects the neighboring helicene molecules resulting in the formation of the superior one-handed helical column with diameter of the hexagonal cavity of 20.533 Å and groove size of 22.226 Å. Second helical assembly formed by CH···π interactions completes hexagonal grove with the outer pitch is about 22.24 Å. (**Figure 4.10)**

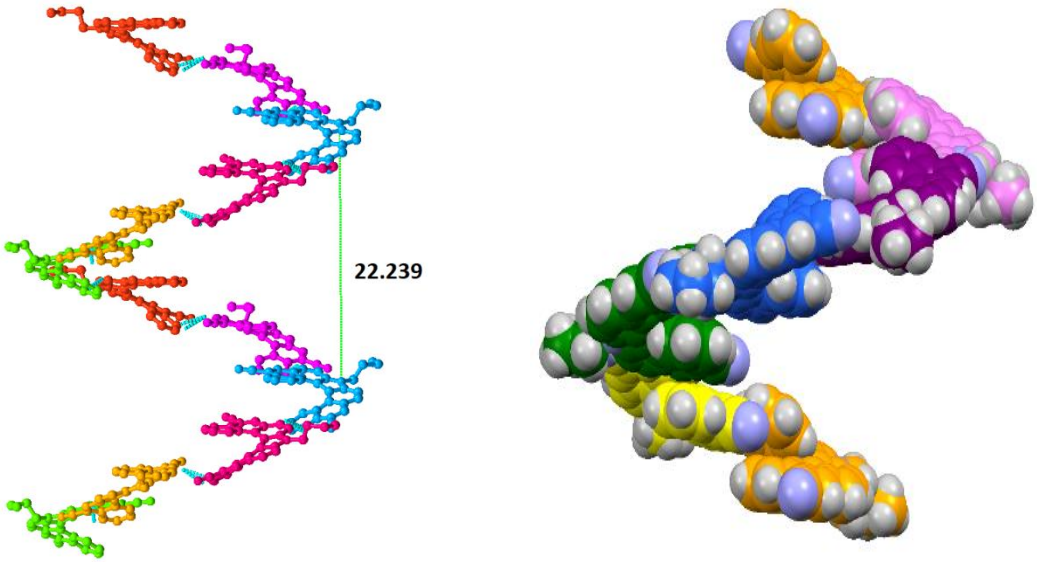

Figure 4.9: Side view of *P*-Super helix arrangement of the conglomerate of (*P*)-**16**. The six molecules forming one turn are given different colors.

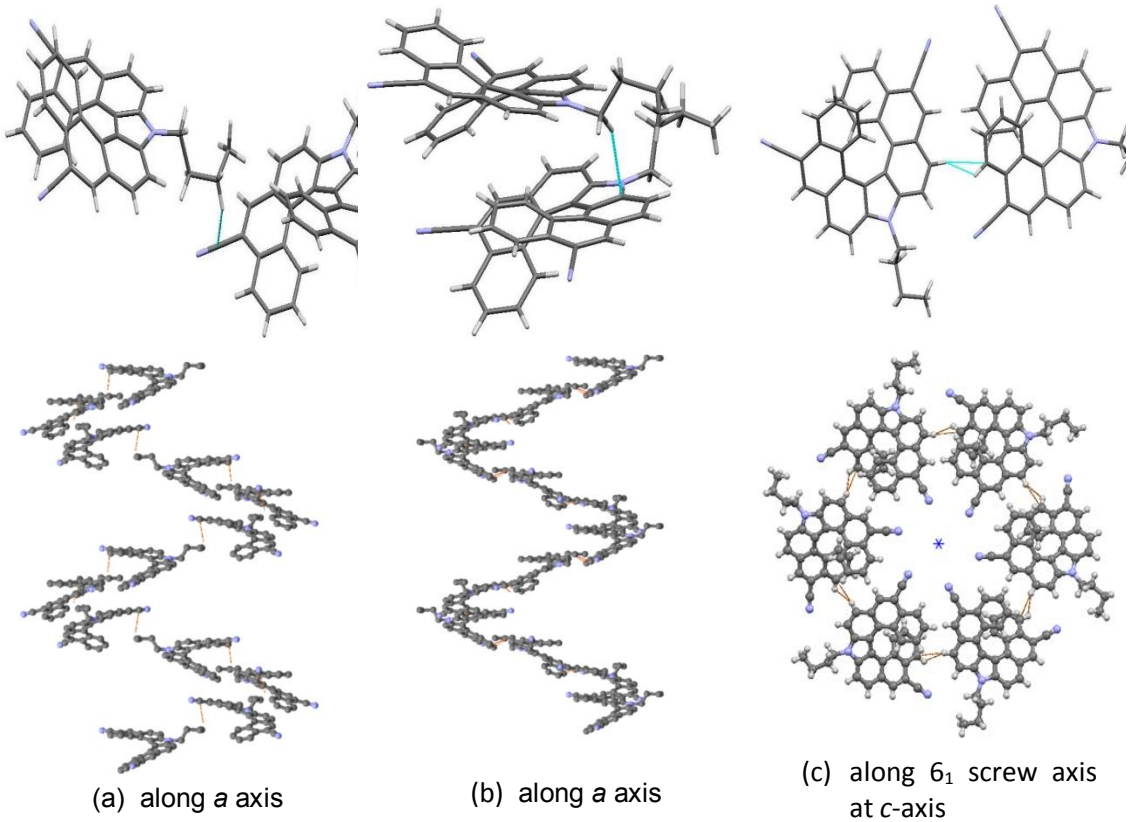

(a) along *a* axis (b) along *a* axis (c) along 6_1 screw axis at *c*-axis

Figure 4.10: Interactions responsible for spontaneous resolution of compound **16**. (a) Hydrogen bonding between -CN and *n*-butyl -CH results into right handed and left handed helical columns (b) CH---π interaction results into right handed and left handed helical columns (c) CH---π interaction results into right handed and left handed helical columns

For each helicene molecule of (*P*)-**16,** the outer pitch of individual molecule is 4.9 Å, while the dihedral angle θ is 35.9° and the distortion of its molecular structure is 46.54°

(φ 1 + φ 2 + φ 3). The other characteristics of such helical structure i.e. lengthening of inside bonds and shortening of outside peripheral bonds were in agreement with the reported values of such molecules. The butyl chain attached to nitrogen also plays a vital role in stabilizing the super helix structure as well as providing adequate solubility of aza[7]helicene in organic solvent. Third helical assembly so formed by supramolecular CH···π interaction of *N*-CH_2- of butyl chain with the carbazole unit of the next strand of the second helical chain molecule holding them tightly. (**Figure 4.10)** Generation of three-fold rotational symmetry of (*P*)-**16** and (*M*)-**16** mediates the helical arrangement by minimizing the vacant void space and by maximizing their aromatic interactions (CH···π). A 6_1 helical axis is passing through the third helical chain/motif made up of CH···π interaction (2.851 Å) with groove size of 22.239 Å.

In addition, it has been observed that (*P*)-**16** [or (*M*)-**16**] helicene aggregate are packed together to form large homochiral supramolecular columns through self-assembly giving directionality and configuration to the helical system. The crystals were recovered after X-ray analysis and their optical rotation and optical purity were measured by HPLC analysis (Chiralpak ODH). The crystal with *P*-helical description showed SOR of +2178 and 76.6 % ee.

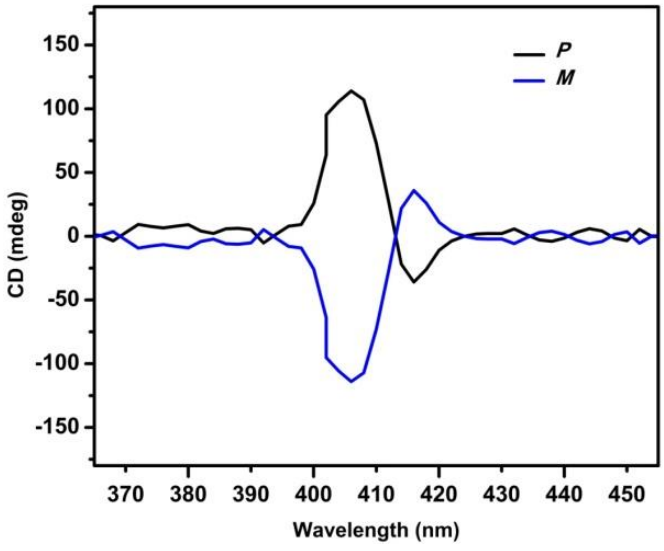

Figure 4.11: CD spectra of compound **16** recorded (*C* = 1.0 X 10^{-5}) in dichloromethane at room temperature.

The crystals of similar diamond shape and dark yellow color were selected and their optical rotations were measured, the correlation of optical purity and SOR values of individual crystals is presented in **Table 4.1**.

No	$[\alpha]_D$ Observed	% ee	$[\alpha]_D$ extrapolated to 100 % ee
1	+2178	76.6	+2895
2	+2507	82.0	+3057
3	+2727	96.7	+2820
4	+2557	85.0	+3008
5	-2927	95.0	-3081
6	-3244	99.0	-3276
7	-3000	98.0	-3061

Table 4.1 Characteristics of some representative crystals

All the crystal parameters of (*P*)-**16** and (*M*)-**16** were almost identical, with for the (±)-**16**. Their CD curves were similar with opposite cotton effect (**Figure 4.11**) The nature of the curves were in accordance to the known aza[7]helicene systems.[34] Thermal behavior of helicene **16** was also investigated by means of differential scanning calorimetry (DSC). The thermogram of racemic and chirally enriched samples differed marginally, indicating different morphology. The sample of (±)-**16** showed slightly lower m.p. (279 ^oC) compared to the crystal of (*P*)-**16** (297 ^oC) and its enantiomer (296 ^oC).[35] The marginal difference between racemic and pure sample is strong indication for the success of conglomerization.

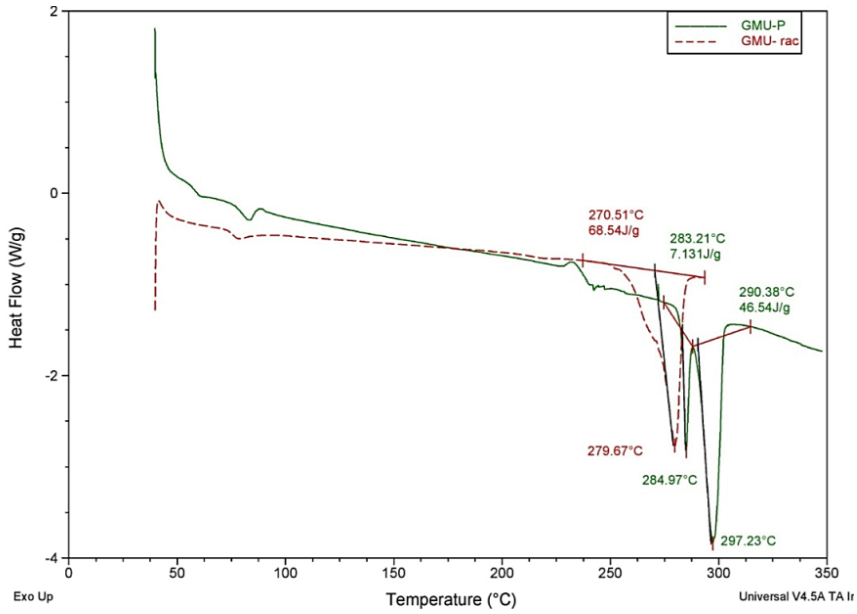

Figure 4.12 Comparison of DSC Thermogram of compound **16**. For Racemic (red) and enriched *P* (green) **Conditions:**Thermogram were recorded under nitrogen atmosphere and ramp were 20°C per min

The difference in physical properties of the chirally pure form, *P* or *M*, with the racemic sample was also evident in the XRD pattern. The compound **16** was configurationally very stable at room temperature. (Qualitative analysis showed that (*M*)-**16** was stable for 24 h when refluxed in toluene; when no racemization was observed)

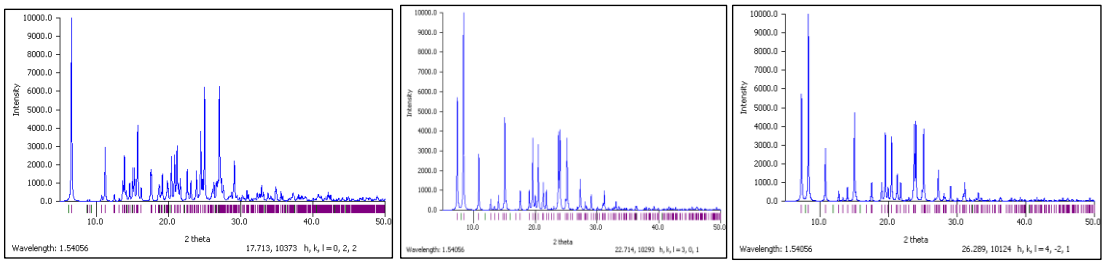

Figure 4.13: Powder XRD data (a) Racemic-**16** (b) ***P*-16** (c) ***M*-16**.

It is quite important to understand the common features of conglomerate formation at the crystallographic level. There is a possibility of a coherent relationship of the substituent on helical framework, ability of molecules of same chiral description to show intermolecular interactions and hence the spontaneous resolution. To study the effect of functional group, their position, effect of side chain and number of cyano groups we studied the crystal interactions of four derivatives of cyano aza[7]helicenes. A systematic comparison of their behavior in crystal structures reveal that the change in

the position of cyano group has a significant effect on molecular recognition. We observe a strong hydrogen bonding between two enantiomers of compound **20** resulting in packing of both (*P*)-**20** and (*M*)-**20** in the unit cell, with intermolecular distance in the range of 2.687 to 2.727 Å. (Figure **4.14**) The butyl chain remains in horizontal position as in compound (±) **16** and forms a CH--π bonding (2.89) with its another isomer and crystallizes as racemic.

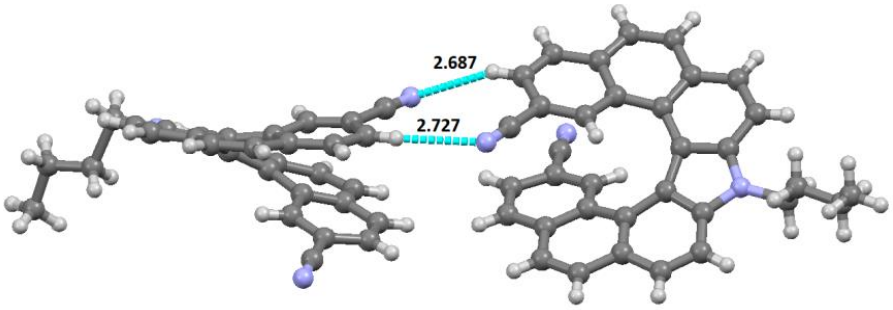

Figure 4.14: CN---H hydrogen bonding between two isomers in **20.**

The compound **17** which has the additional methoxy group at 2 and 16 position showed interesting crystal arrangement as of (*P*)-**16**/(*M*)-**16**. Although, **17** shows favorable stacking interactions like **16**, but slightly weaker Ar-H·····N≡C (as the Ar-H is less δ^+), where racemic crystals were obtained. (Figure **4.15**)

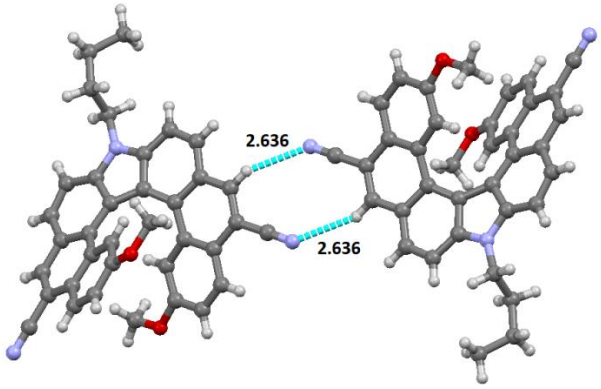

Figure 4.15 CN--H hydrogen bonding between two isomer of **17**.

The additional cyano group in tetracyano **18** drastically affects its solubility in organic solvents and we could not grow a good quality crystal for its study of interactions. Further we introduced a phenyl group in the side chain in **19** hoping that the additional CH–π, π–π interactions will improve its recognition ability, also to check the role of butyl chain and its influence on the magic angle. In the crystal, the(*P*)-**19** recognizes another isomer (*M*)-**19** by strong π–π bonding (**Figure 4.16**) phenyl ring in the side

chain showed the CH-π bonding with another isomer leading to co-crystallization. The isomer also forms strong intermolecular H-bonding between Ar-CN·····H-Ar (2.653Å) (**Figure 4.16b**)

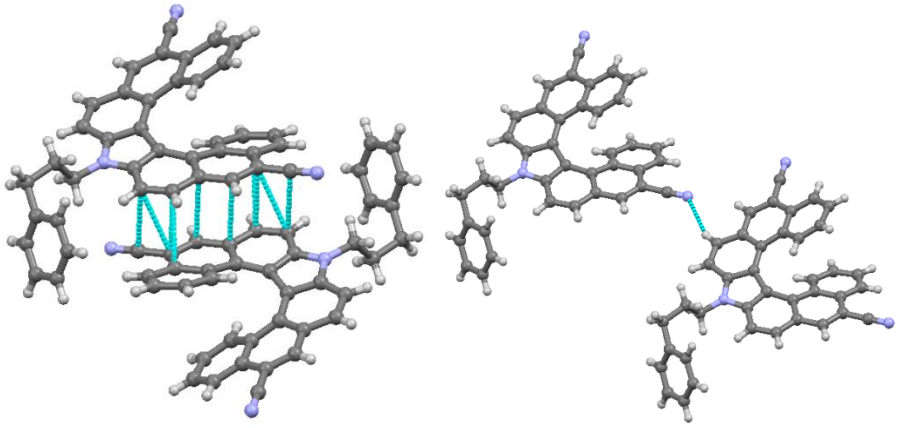

Figure 4.16: (a) π–π stacking in helicene with opposite isomer of **4d. (b)** H-bonding between Ar-CN·····H-Ar

4.8 Attempts towards the peripheral modification of cyano aza[7]helicenes:

The crystals structure of compound **17** showed no enantio-enrichment even though it had the presence of all desired interactions, as in case of compound **16**. Although it was not a complete failure, the SOR values of individual crystals dissolved in dichloromethane reflected some degree of enrichment. Unfortunately the results were non reproducible and the crystal structure was found to contain the well-defined stacking of enantiomers but with the opposite isomer. These results are contradictory to the work by Tanaka *et al* [36] on the thiahelicenes. They found that the methoxy derivatives showed conglomerate behavior while the demethylated hydroxy helicene crystallized as racemate. We believed the presence of polar group with additional H bonding capabilities may enhance the ability to show spontaneous resolution. This made us curious to check the crystallization behavior of hydroxy cyano aza[7] helicene **21**.

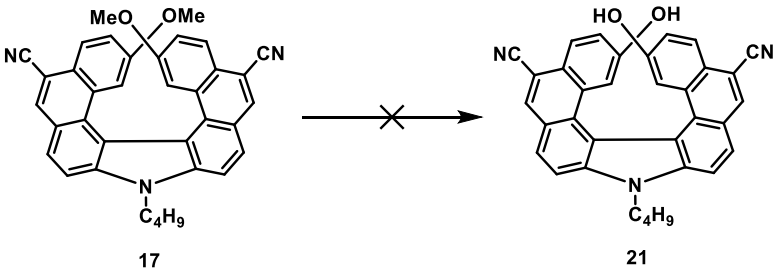

Scheme 4.3: Attempted synthesis of hydroxy cyano aza[7]helicene **21**.

We attempted many methods to convert compound **17** into compound **21** using various reagents such as BBr_3, HBr-AcOH, pyridine-hydrochloride, $AlCl_3$, LiBr-molecular sieves etc but none of them gave the desired material.

In a different approach we wanted to check the effect of position of cyano group on different locations of the helical framework. The presence of cyano functionality on 5th carbon position consistently gave us the conglomerate crystals as in case of compound **16**. We considered to incorporate –CN group on 6th carbon of helical skeleton and to test this molecule for spontaneous resolution. The retro-synthetic analysis was to make the 3, 6-bis cyano methyl carbazole as the starting material followed by Knovenagel condensation to give bis-styryl derivative and the last step to carry out photocyclization to install cyano group on the desired site.

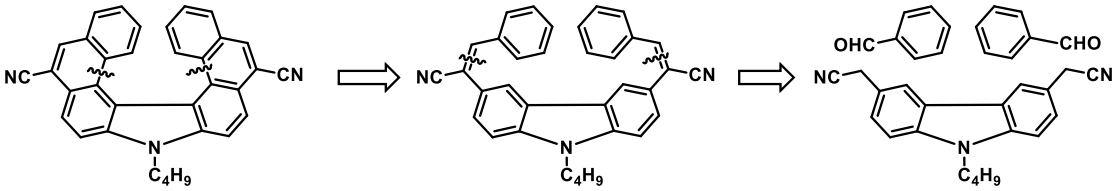

Scheme 4.4: Retrosynthetic analysis of compound **22**.

The attempted synthetic route for the preparation of compound **22** is presented in scheme **4.5** where 3, 6 –diformyl carbazole **23** was reduced to 3, 6-dihydroxy methyl carbazole **24** using $NaBH_4$ in methanol-dichloromethane solvent mixture. The compound **24** was then subjected to bromination using aqueous HBr at 0^{o}C to get dibromo methyl carbazole **25**. Our attempts to isolate and characterize compound **25** were not successful. The transformation of hydroxyl group of compound **24** in to corresponding bromide, mesylate or tosylate failed probably due to high reactivity of products, which undergoes fast polymerization. To address the stability issue of compound **25** we have taken KCN in the same flask hoping the unstable dibromo compound **25** will react *in situ* with it. to give the desired dicyano methyl carbazole however the outcome remained same.

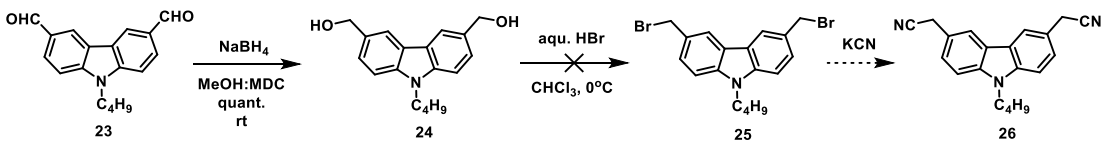

Scheme 4.5: Attempted synthesis of dicyano methyl carbazole.

A different synthetic route for the preparation of compound **22** was adopted (**Scheme 4.6**). We began our synthesis by accessing stilbene derivative **29** by Knoevenagel condensation of benzaldehyde and *p*-methoxy benzyl cyanide **27**. The photo induced oxidative cyclization of **29** gave us the phenanthrene derivative **30** in quantitative conversion.

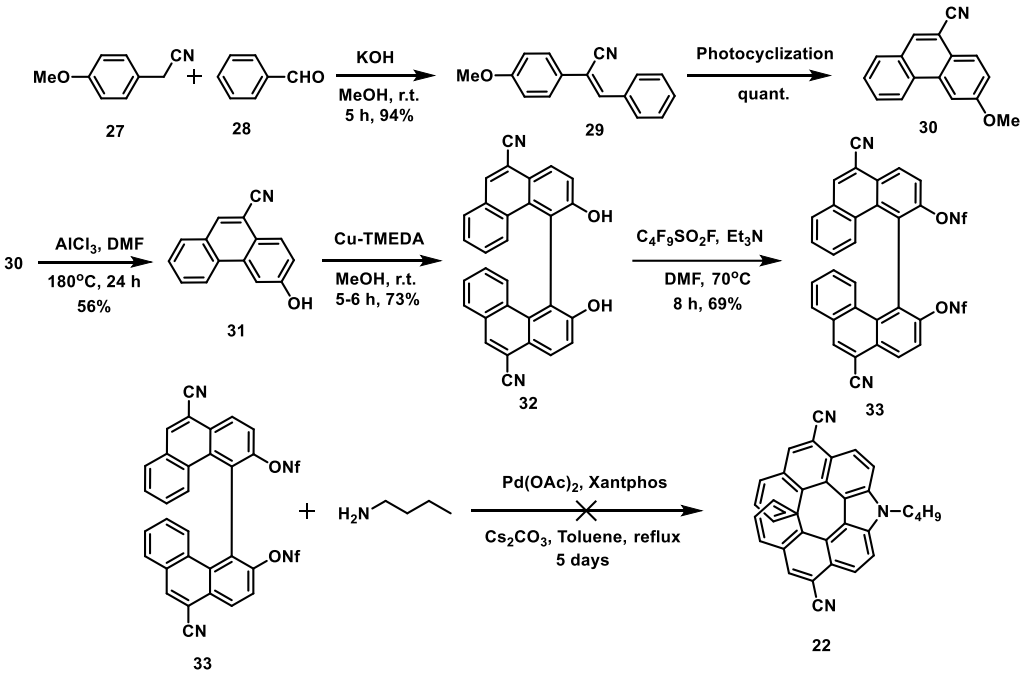

Scheme 4.6. Attempted synthesis of compound **22**.

In the next step we needed to cleave the methyl ether to access phenol **31**. It was achieved using $AlCl_3$ in DMF at 180°C. The phenol **31** was then subjected to oxidative coupling using Cu-TMEDA, in methanol at ambient conditions to afford the dihydroxy derivative **32** in 73% yield. The dihydroxy compound **32** was converted to its di-nonafluoro sulfonate **33** by the reaction with pernonafluoro sulfonyl fluoride in DMF. The compound **33** was then subjected to double *N*-arylation reaction using butyl amine with palladium acetate-Xantphos system. Unfortunately the reaction did not take place even heating for prolonged time (5 days). Thus we could not synthesize the desired target molecule for screening its crystallization behavior.

4.9 Conclusion:

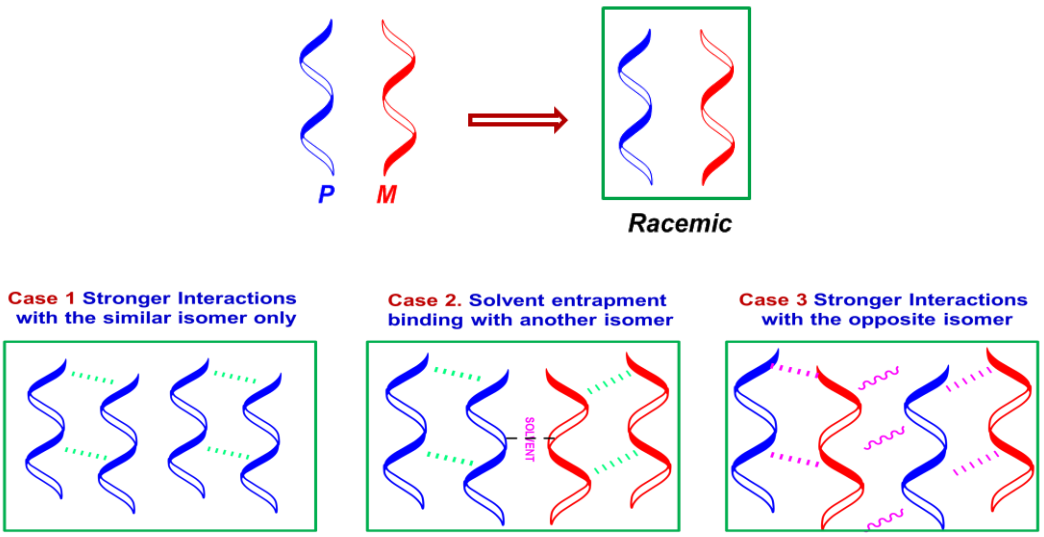

The aim of this work was to prove the –CN to be an ideal synthon for the process of spontaneous resolution and to provide a generalized idea that the presence of cyano group can leads to conglomerization process with consistency. For this purpose five derivatives of cyano aza[7]helicene have been synthesized and screened for their crystallization behavior. The crystallization behavior of these five derivatives can be classified into three cases.

Case 1: The successful candidate 5, 13-dicyano aza[7]helicene **16** when crystallized from 1, 2-dichloroethane, gave enantio enriched crystals by making stronger CN…H-Ar interactions along by means of other favorable interactions with the isomer of same chirality, crystallizing out as pure enantiomer.

Case 2: The same compound **16** when crystallized in dichloromethane, formed similar contacts as it was crystallized using dichloroethane except the solvent entrapped in the crystal lattice. The entrapped solvent act as binder between the stacks of isomers of opposite chirality ultimately leading to the racemic mixture.

Case 3: The behavior of other four derivatives **17-20** as they contain similar –CN groups, butyl side chain and also everything were placed appropriately to make desired contacts. The crystals structure revealed identical stacking and interactions with the isomer of similar chirality as that of successful candidate **16**. The only difference was the formation of additional strong interactions with the isomer of opposite chirality leading to crystallization as racemic mixture.

We conclude that the success of spontaneous resolution depends on the ability of molecules to form right kind of contacts among the neighbor of the same chirality. Any factor that alters this ability of a molecule either by weakening the interactions to identify its partner (similar isomer) or by making stronger interactions with the opposite isomer; decreases the chiral recognition property of a molecule. These crystallographic comparisons suggest that the presence of dipole−dipole interactions are essential but not enough for making the right contacts with the neighboring molecule of the same handedness, which is required for spontaneous resolution. We believe these findings will contribute to the general understanding of the relatively uncommon phenomena of spontaneous resolution by conglomerate formation and can lead to more success in this aspect of crystal engineering and supramolecular interactions in solids.

4.10 Few prominent interactions:

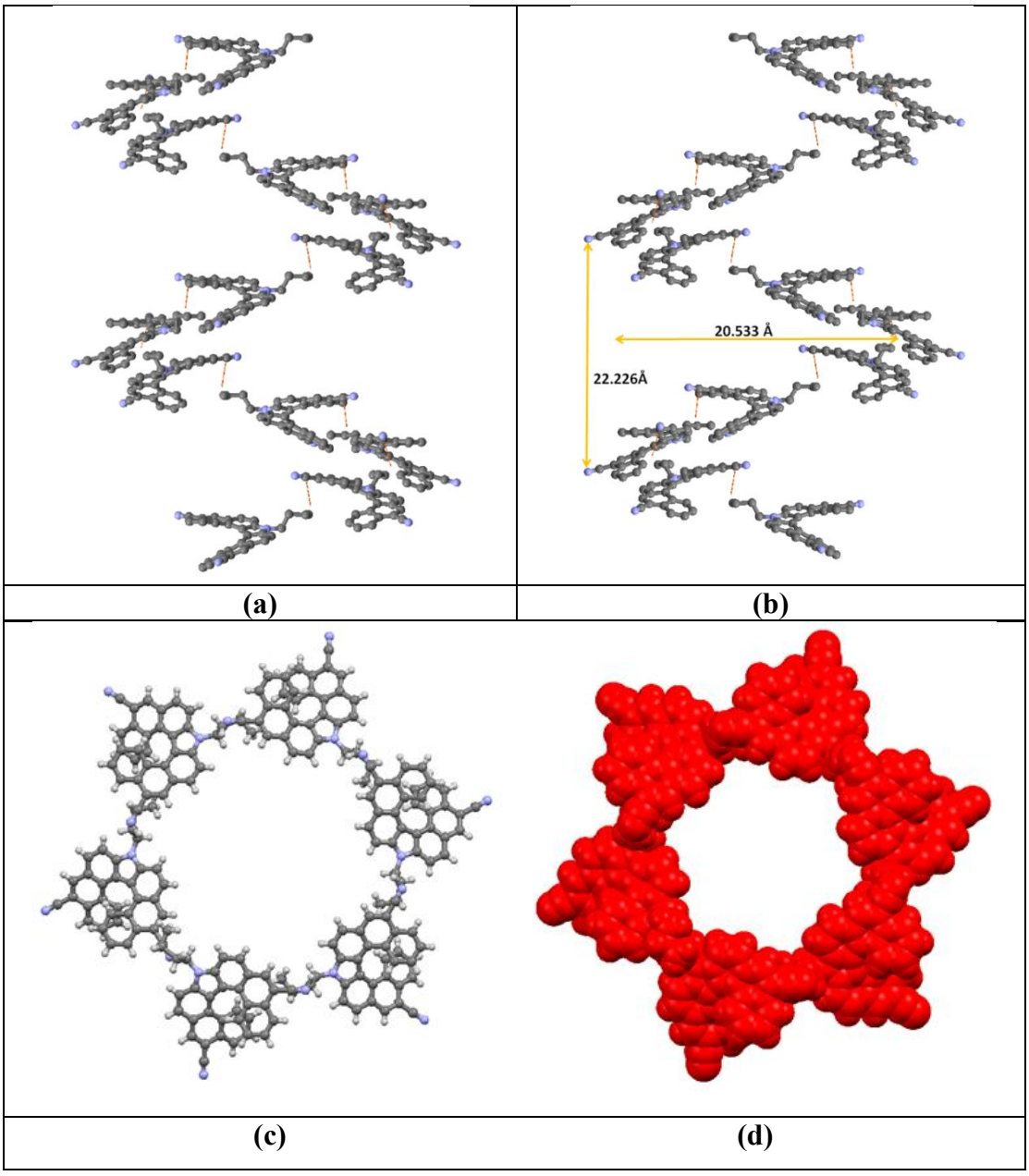

Figure 4.16:.(a) and (b) Hydrogen bonding between -CN and *n*-butyl -CH results into right handed and left handed helical columns along *a*-axis respectively; (c) and (d) CN···H interactions helical column along 6_1 screw axis at *c*-axis. (compound **16**)

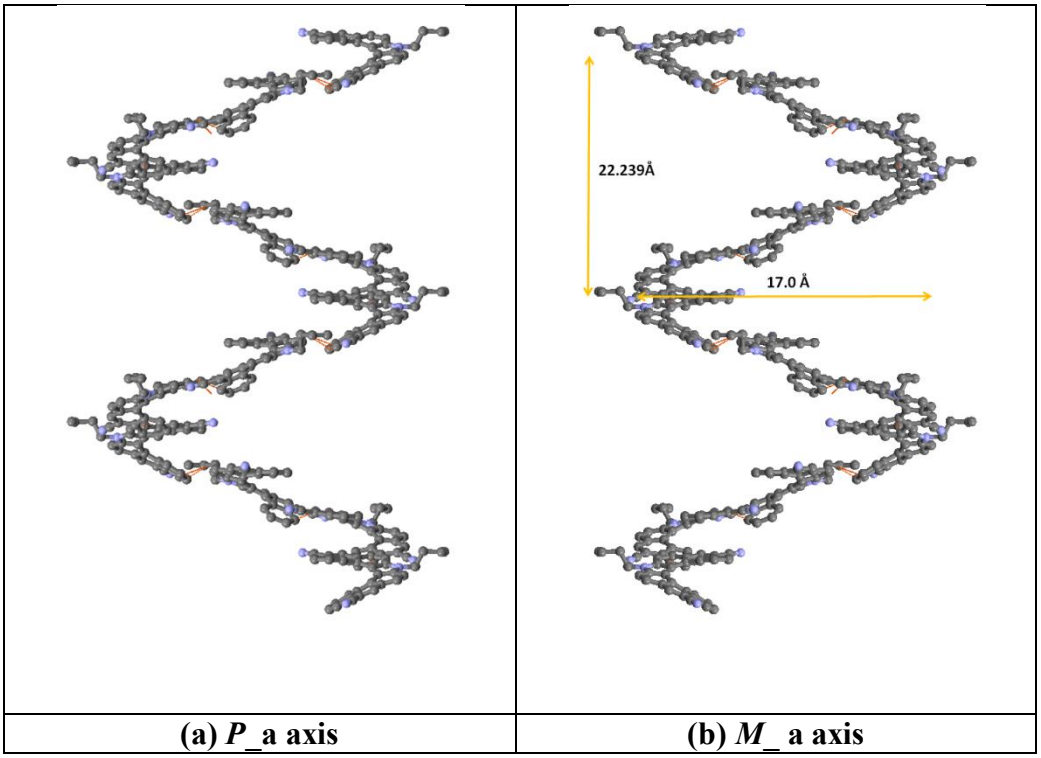

Figure 4.17: (a) and (b) CH---π interaction results into right handed and left handed helical columns along *a*-axis respectively; (c) CH---π interaction helical column along 6_1 screw axis at *c*-axis and (d) and (e) First helical and second helical strands. (Compound **16**)

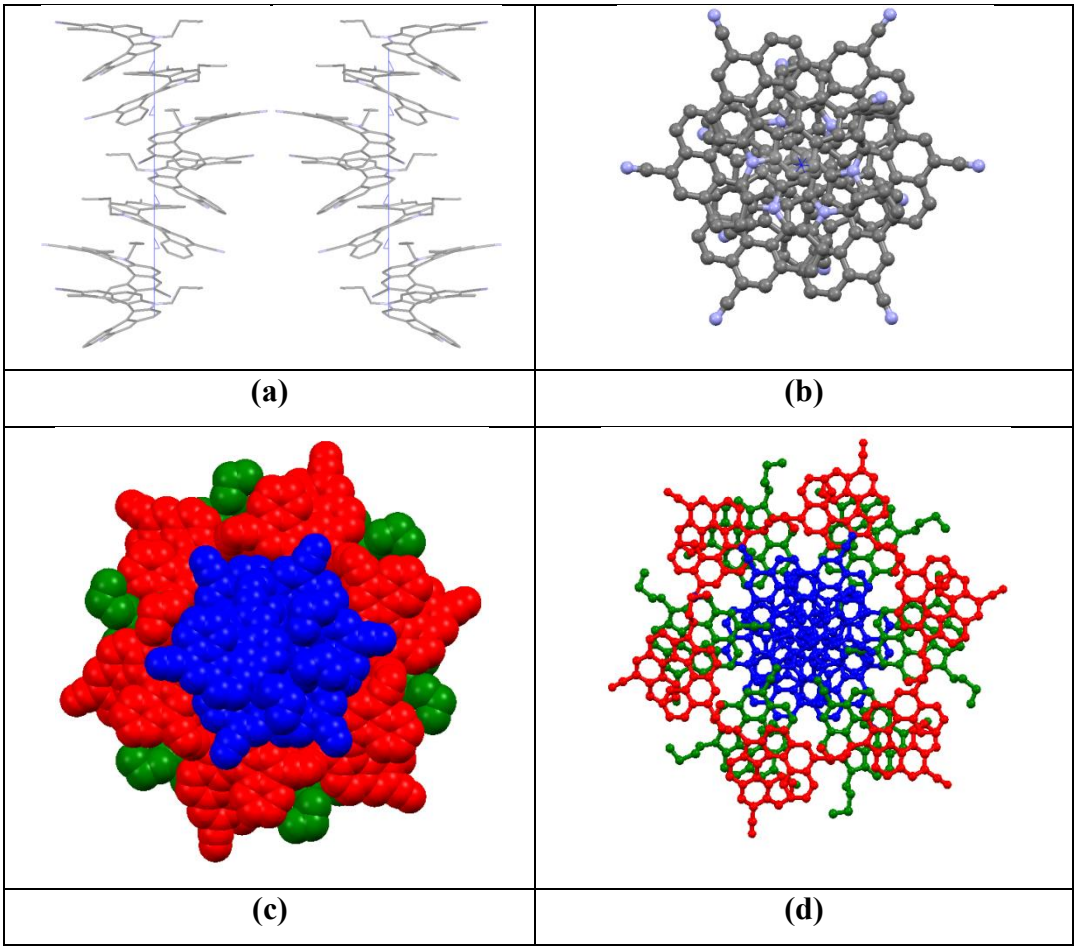

Figure 4.18: (a) CH---π interaction results into right handed and left handed helical columns along *a*-axis respectively; (b) CH---π interaction helical column along 6_1 screw axis at *c*-axis and (d) and (e) All three helical strands together (compound **16**).

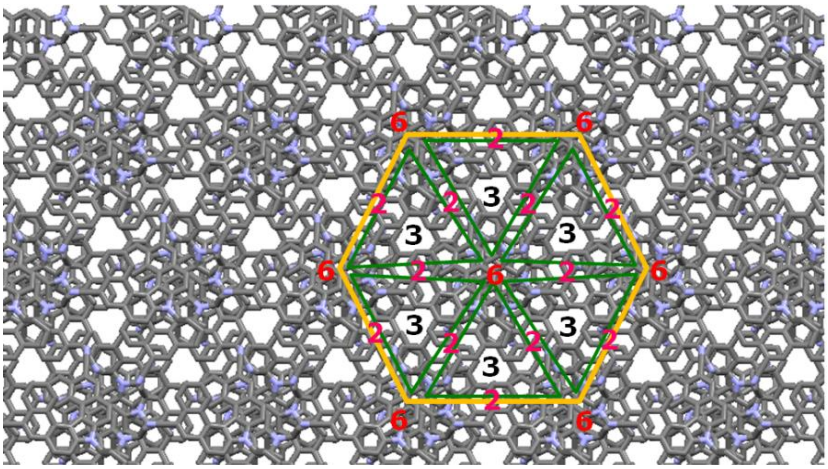

Figure 4.19:. Honeycomb net-like network with the representation of six-fold, three-fold and two-fold axis position in hexagon (compound **16**).

4.11 X-ray crystal data:

Identification code	***P/M*-16**	***P*-16**	***M*-16**
CCDC No.	**1019783**	**1410010**	**1019782**
Empirical formula	$C_{35}H_{25}Cl_2N_3$	$C_{34}H_{23}N_3$	$C_{34}H_{23}N_3$
Formula weight	558.48	473.55	473.55
Temperature/K	120(2)	293(2)	293(2)
Crystal system	Monoclinic	Hexagonal	Hexagonal
Space group	$P2_1/c$	$P6_1$	$P6_5$
a/Å	13.4117(3)	13.8475(4)	13.8494(5)
b/Å	14.1188(3)	13.8475(4)	13.8494(5)
c/Å	14.2602(3)	22.2392(5)	22.2255(7)
α/°	90.00	90.00	90.00
β/°	93.694(2)	90.00	90.00
γ/°	90.00	120.00	120.00
Volume/Å^3	2694.66(10)	3693.09(16)	3691.8(2)
Z	4	6	6
ρ_{calc}g/cm^3	1.377	1.278	1.278
μ/mm^{-1}	2.399	0.583	0.584
F(000)	1160.0	1488.0	1492.0
Crystal size/mm^3	0.20 × 0.20 × 0.18	0.70 × 0.68 × 0.60	0.20 × 0.19 × 0.15
Radiation (CuKα)	1.54184	1.54184	1.54184
2Θ range for data collection/°	6.6 to 146.6	13.4 to 145.6	7.38 to 146.44
Index ranges	$-16 \le h \le 16$, $-11 \le k \le 17$, $-17 \le l \le 17$	$-14 \le h \le 17$, $-14 \le k \le 17$, $-18 \le l \le 27$	$-13 \le h \le 14$, $-14 \le k \le 14$, $-27 \le l \le 15$
Reflections collected	17149	14181	9342
Data/restraints/parameters	5417/0/362	4904/1/336	3076/1/335
Goodness-of-fit on F^2	1.044	1.047	1.050
Final R indexes [I>=2σ (I)]	R_1 = 0.0571, wR_2 = 0.1602	R_1 = 0.0577, wR_2 = 0.1556	R_1 = 0.0555, wR_2 = 0.1411
Final R indexes [all data]	R_1 = 0.0609, wR_2 = 0.1662	R_1 = 0.0620, wR_2 = 0.1601	R_1 = 0.0758, wR_2 = 0.1536
Largest diff. peak/hole / e Å^{-3}	0.94/-0.43	0.35/-0.32	0.25/-0.22
		0.05(11)	-0.1(12)

Identification code	**17**	**20**	**19**
CCDC No.	**1846027**	**1511883**	**1854223**
Empirical formula	$C_{36}H_{27}N_3O_2$	$C_{34}H_{23}N_3$	$C_{39}H_{25}N_3$
Formula weight	533.61	473.55	535.62
Temperature/K	293(2)	293(2)	293(2)
Crystal system	monoclinic	orthorhombic	orthorhombic
Space group	$P2_1/c$	$Pca2_1$	Pbca
a/Å	8.2152(6)	27.1157(14)	13.952(4)
b/Å	21.4774(11)	13.4939(11)	13.952(4)
c/Å	15.9373(9)	13.5188(7)	28.689(13)
α/°	90.00	90.00	90.00
β/°	104.863(7)	90.00	90.00
γ/°	90.00	90.00	90.00
Volume/Å^3	2717.9(3)	4946.5(5)	5585(3)
Z	4	8	8
ρ_{calc}g/cm^3	1.304	1.272	1.274
μ/mm^{-1}	0.082	0.581	0.075
F(000)	1120.0	1984.0	2642.0
Crystal size/mm^3	0.32 × 0.28 × 0.26	0.30 × 0.11 × 0.10	0.43 × 0.32 × 0.23
Radiation	MoKα (λ = 0.71073)	CuKα (λ = 1.54184)	MoKα (λ = 0.71073)
2Θ range for data collection/°	6.28 to 57.98	9.24 to 142.76	6.38 to 58.9
Reflections collected	10133	12192	23242
Data/restraints/parameters	7224/0/373	9636/1/669	6339/0/380
Goodness-of-fit on F^2	1.017	1.050	0.928
Final R indexes [I>=2σ (I)]	R_1 = 0.0426, wR_2 = 0.0986	R_1 = 0.0601, wR_2 = 0.1298	R_1 = 0.0835, wR_2 = 0.1285
Final R indexes [all data]	R_1 = 0.0646, wR_2 = 0.1097	R_1 = 0.1015, wR_2 = 0.1583	R_1 = 0.2787, wR_2 = 0.1965
Largest diff. peak/hole / e Å^{-3}	0.16/-0.13	0.28/-0.18	0.25/-0.15

4.12 Experimental procedures:

9-(3-Phenyl propyl)-3,6-diformyl carbazole:

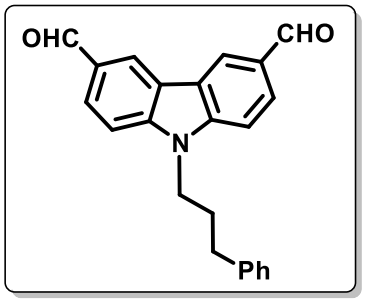

Phosphoryl chloride (10.76 g, 6.56 mL, 70.1 mmol) was added slowly in dry DMF (5.11 g, 5.38 mL, 70.1 mmol) which was purged with nitrogen and cooled at 0 °C. The reactant was warmed at room temperature, stirred for 1h and then cooled again for 0 °C. To this mixture was added *N*-(3-phenyl propyl) carbazole (2.0 g, 7.01 mmol) in dichloroethane (25 mL). In 1h, the reaction temperature was raised to 90 °C and then kept for 8 h. After the completion of the reaction, the mixture was poured into ice-cold water and extracted with dichloromethane (3 x 100 mL). The combined organic phase was washed with water, brine, and dried over anhydrous sodium sulfate. The solvent was removed under reduced pressure and the crude product was purified by column chromatography on silica gel using petroleum ether–ethyl acetate (70:30) as eluent to afford of 9-(3-phenyl propyl) 3,6-diformyl carbazole as brown solid (1.22 g, 51%).

^{1}H-NMR (400 MHz, $CDCl_3$): δ 10.14 (s, 2H), 8.66 (d, *J* = 1.2 Hz, 2H), 8.07 (dd, *J* = 8.4 and 1.2 Hz, 2H), 7.44 (d, *J* = 8.4 Hz, 2H), 7.35-7.31 (m, 2H), 7.28-7.20 (m, 3H), 4.40 (t, *J* = 7.2 Hz, 2H), 2.76 (t, *J* = 7.6 Hz, 2H), 2.28 (quint, *J* = 7.6 Hz, 2H)

3,6-Diformyl-9-butyl-9*H*-carbazole:

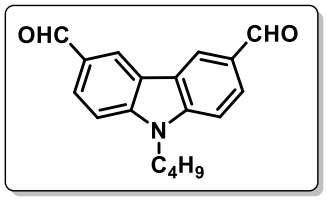

Synthetic procedure is similar to described for the synthesis of 9-(3-phenyl propyl) 3,6-diformyl carbazole.

m.p. = 130-133 °C.

Yield = 71%

^{1}H-NMR (400 MHz, $CDCl_3$): δ = 10.14 (s, 2H), 8.68 (d, *J*= 1.2 Hz, 2H), 8.09 (dd, *J* = 8.4 and 1.2 Hz, 2H), 7.56 (d, *J* = 8.4 Hz, 2H), 4.40 (t, *J* = 7.2 Hz, 2H), 1.93 - 1.88 (m, 2H), 1.46 - 1.40 (m, 2H), 0.98 (t, *J* = 7.6 Hz, 3H).

General procedure for the synthesis of carbazole derived stillbene derivative by Knovenagel reaction:

3,3-(9-Butyl-9*H*-carbazole-3,6-diyl)-bis(2-phenylacrylonitrile) (15): A solution of 9-butyl carbazole-3,6-dicarbaldehyde (1.0 g, 3.58 mmol) and phenylacetonitrile (1.04 g, 8.96 mmol) in dry ethanol (25 mL) was placed in a single neck R.B. flask fitted with a septum , which is degassed and purged with nitrogen. To this was added drop-wise, with stirring, a solution of (0.824 g, 35.8 mmol) sodium dissolved in 25 mL of dry ethanol and the mixture was stirred vigorously for 6 hours at room temperature. After completion of reaction the ethanol was evaporated under reduced pressure the mixture was poured into ice-cold water and extracted with ethyl acetate (3 x 100 mL). The combined organic phase was washed with water, brine, and dried over anhydrous sodium sulfate. The solvent was removed under reduced pressure and the crude product was purified by column chromatography on silica gel using petroleum ether–ethyl acetate (90:10) as eluent to afford **15**. (1.47 g, 86%) as yellow solid. m.p. = 192-194 ^{o}C

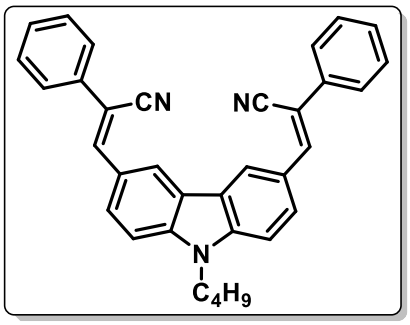

^{1}H-NMR (400 MHz, CDCl$_3$): δ 8.65 (s, 2H), 8.24 (dd, *J* = 8.4 Hz and 1.6 Hz, 2H), 7.76-7.74 (m, 6H), 7.52-7.47 (m, 6H), 7.43-7.39 (m, 2H), 4.37 (t, *J* = 7.2 Hz), 1.95-1.88 (m, 2H), 1.49-1.39 (m, 2H), 1.0 (t, *J* = 7.2 Hz, 3H).

^{13}C-NMR (100 MHz, CDCl$_3$):δ 143, 142, 135, 129, 128.6, 127.4, 125.8, 125.7, 123.1, 122.9, 118.9, 109.6, 108.2, 43.3, 31.1, 20.5, 13.8.

IR (KBr): 2927, 2857, 2234, 1634, 1557, 1285, 1243, 1155, 907, 803, 749, 694 cm^{-1}

HRMS (ESI): *m/z* calculated for $C_{34}H_{27}N_3Na$ $[M+Na]^+$: 500.2096; found; 500.2097.

3,3-(9-Butyl-9*H*carbazole-3,6-diyl)-bis(2-(4-methoxyphenyl)acrylonitrile) (15 a):

Yield= 86 %; Physical state = Yellow solid; m.p. =181-183 ^{o}C

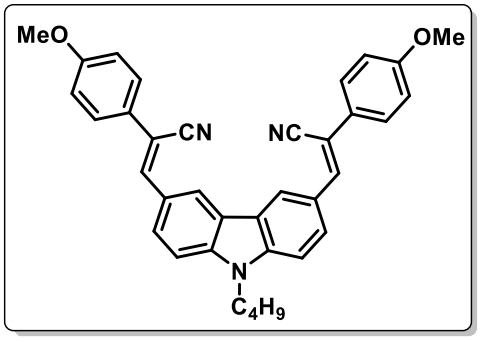

^{1}H-NMR (400 MHz, CDCl$_3$): δ 8.60 (d, 2H), 8.20-8.17 (m, 2H), 7.69-7.63 (m, 6H), 7.51-7.47 (m, 2H), 7.0 (dd, *J* = 8.8 Hz and *J* = 1.6 Hz, 4H), 4.34 (t, *J* = 7.2 Hz, 2H), 3.89 (s, 6H), 1.92-1.86 (m, 2H), 1.61-1.39 (m, 2H), 0.99 (t, *J* = 7.6 Hz, 3H);

^{13}C-NMR (100 MHz, CDCl$_3$): δ 160.0, 141.8,

141.1, 127.5, 127.1, 127.0, 125.9, 123.0, 122.6, 119.1, 114.4, 109.5, 107.8, 55.4, 43.3. 31.1, 20.5, 13.8.

IR (KBr): 2932, 2207, 1666, 1601, 1509, 1291, 1247, 1178, 1028, 904, 826 cm^{-1}

HRMS (ESI): *m/z* calculated for $C_{36}H_{31}N_3O_2Na$ $[M+Na]^+$: 560.2308; found; 560.2305.

4, 4'-((9-Butyl-9H-carbazole-3,6-diyl)bis(1-cyanoethene-2,1-diyl))dibenzonitrile (15b):

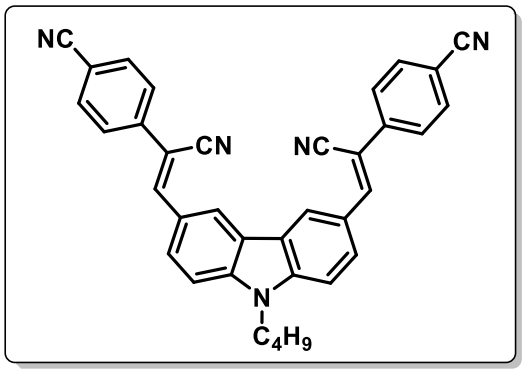

Yield = 51 %; Physical state = Light Orange solid; m.p. => 250 °C

^{1}H-NMR (400 MHz, $CDCl_3$): δ 8.73 (s, 2H), 8.22 (d, *J* = 8.0 Hz, 2H), 7.85-7.83 (m, 6H), 7.77-7.75 (m, 4H), 7.55 (d, *J* = 8.8 Hz, 2H), 4.39 (t, *J* = 6.8 Hz, 2H), 1.94-1.88 (m, 2H), 1.49-1.41 (m, 2H), 1.00 (t, *J* = 7.2 Hz, 3H) .

^{13}C-NMR (100 MHz, $CDCl_3$): δ 145.3, 142.7, 139.3, 132.8, 128.3, 126.1, 125.2, 123.3, 123.2, 118.4, 118.1, 112.0, 110.0, 106.4, 43.5, 31.1, 20.5, 13.8.

IR (KBr): 3049, 2821, 2801, 2229, 2209, 1631, 1582, 1487, 1413, 921, 840 cm^{-1};

HRMS (ESI): *m/z* calculated for $C_{36}H_{25}N_5Na$ $[M+Na]^+$: 550.1996; found; 550.2002.

3,3'-(9-(3-Phenylpropyl)-9*H*-carbazole-3,6-diyl) bis(2 phenylacrylonitrile) (15c): Yield = 51% Physical State = yellow solid m.p.: 144 °C.

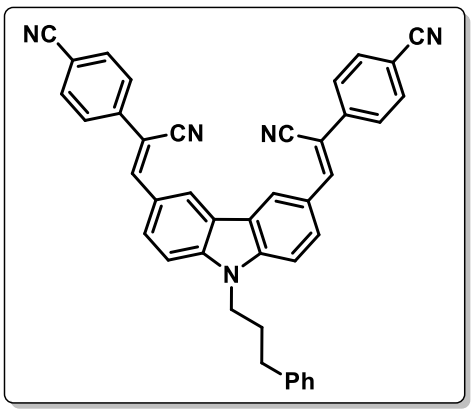

^{1}H-NMR (400 MHz, $CDCl_3$): δ 8.64 (d, *J* = 1.6 Hz, 2H), 8.20 (dd, *J* = 8.8 and 1.6 Hz, 2H), 7.75-7.73 (m, 6H), 7.51-7.43 (m, 4H), 7.42-7.33 (m, 6H), 7.28-7.27 (m, 4H), 4.35 (t, *J* = 7.2 Hz, 2H), 2.76 (t, *J* = 7.2 Hz, 2H), 2.27 (quint, *J* = 7.6 Hz, 2H).

^{13}C-NMR (100 MHz, $CDCl_3$): δ 142.9, 141.9, 140.4, 134.9, 129.0, 128.7, 128.6, 128.3, 127.4, 126.4, 125.8, 125.7, 123.1, 122.9, 118.9, 109.5, 108.2, 42.8, 33.1, 30.0.

IR (KBr): 2925, 2851, 2229, 1637, 1567, 1281, 1243, 1155, 907, 803, 743, 691 cm^{-1}

HRMS: (ESI): *m/z* calculated for $C_{39}H_{29}N_3Na$ $[M+Na]^+$: 562.2254; found; 562.2253.

3,6-Bis-(4-cyano styryl)-*N*-butyl carbazole (15d):

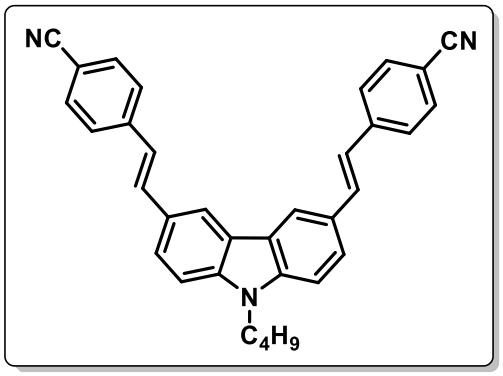

A solution of palladium acetate (0.009 g, 0.042 mmol, 2 mol %) and 1, 3-bis(diphenylphosphinopropane) (0.034 g, 0.084 mmol, 4 mol %) was prepared in *N*,*N*-dimethylacetamide (5 mL) under nitrogen atmosphere. The mixture was stirred at room temperature until a homogeneous solution was obtained.

This catalyst solution was repeatedly purged by N_2 prior to use. A two-necked round bottom flask was charged with 3,6-diiodo-*N* butylcarbazole(1.0 g, 2.1 mmol), dry potassium carbonate (1.16 g, 8.4 mmol), TBAB (0.135 g, 0.42 mmol, 20 mol %), and *N*,*N*-dimethylacetamide (10 mL). The solution was repeatedly purged with N_2 *p*-cyano styrene (0.59 g, 4.63mmol) was added at 60°C and the mixture was heated up to 100°C. At 100°C, the previously prepared Pd catalyst solution was added drop wise and the mixture was further heated to 140°C for 48 h. After the completion of the reaction, the mixture was poured into ice-cold water and extracted with dichloromethane (3 x 100 mL). The combined organic phase was washed with water, brine, and dried over anhydrous sodium sulfate. The solvent was removed under reduced pressure and the crude product was purified by column chromatography on silica gel using petroleum ether–ethyl acetate (80:20) as eluent to afford3, 6-bis-(4-cyano styryl)-*N*-butyl carbazole. **15d** as yellow solid (0.81 g, 81%). m.p. = 239-240 °C

^{1}H-NMR (400 MHz, $CDCl_3$): δ 8.30 (d, *J* = 1.2 Hz, 2H), 7.72 (dd, *J* = 8.4 Hz and *J* = 1.6 Hz, 2H), 7.68-7.63 (m, 8H), 7.47-7.43 (m, 4H), 7.16 (d, *J* = 16.4 Hz, 2H), 4.35 (t, 6.8 Hz, 1.94-1.86 (m, 2H), 1.48-1.39 (m, 2H), 0.98 (t, *J* = 7.6 Hz, 3H)

^{13}C-NMR (100 MHz, $CDCl_3$): δ 142.6, 141.3, 133.3, 132.6, 128.1, 126.6, 125.3, 124.4, 123.4, 119.5, 119.3, 110.0, 109.5, 43.3, 31.3, 20.6, 14.0

IR (KBr): 2954, 2925, 2220, 1591, 1484, 1247, 1210, 960, 859, 819 cm^{-1}

HRMS (ESI): *m/z* calculated for $C_{34}H_{27}N_3Na$ $[M+Na]^+$: 500.2097; found; 500.2105.

Typical procedure for photocyclization:

***N*-butyl 5,13-dicyano aza[7]helicene (16):**

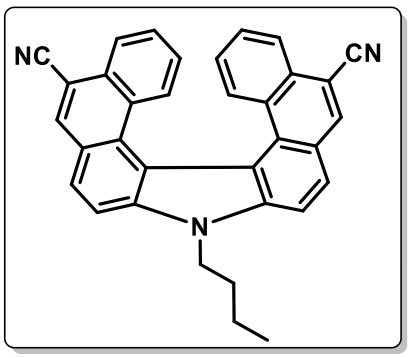

In an immersion wall photo reactor (borosilicate glass) equipped with a water cooling jacket and stir bar a solution of 3,3-(9-butyl-9*H*carbazole-3,6-diyl)-bis(2-phenylacrylonitrile) **15** (0.2 g, 0.42 mmol), iodine (0.185 g, 0.73 mmol), THF (3.02 g, 3.40 mL, 42.0mmol) and toluene (350 mL) was irradiated using a 125W HPMV lamp for 7 h monitored by TLC. After the completion of reaction, the excess of iodine was removed by washing the solution with aqueous $Na_2S_2O_3$, followed by distilled water. The organic layer was concentrated under the reduced pressure to obtain the crude product. The crude product purified by column chromatography over silica gel using petroleum ether: ethyl acetate (80:20) as eluent to obtained compound **16** as yellow solid (0.173 g, 86%), m.p. = *rac*-279 ^oC, *M*- isomer =297 ^oC

^{1}H-NMR (400 MHz, $CDCl_3$): δ 8.50 (s, 2H), 8.22 (d, *J* = 8 Hz, 2H), 8.13 (d, *J* = 8.4 Hz, 2H), 8.01 (d, *J* = 8.8 Hz, 2H), 7.34-7.31 (m, 2H),7.16 (d, *J* = 8Hz, 2H), 6.27-6.23 (m, 2H), 4.77 (t, *J* = 7.6 Hz, 2H), 2.13-2.05 (m, 2H), 1.69-1.52 (m, 2H), 1.05 (t, *J* = 7.6Hz,3H)

^{13}C-NMR (100 MHz, $CDCl_3$): δ 141.0, 135.3, 129.2, 128.7, 128.3, 127.9, 127.8, 127.7, 124.8, 124.1, 123.8, 118.6, 116.2, 110.9, 105.9, 43.7, 31.8, 20.6, 13.9

IR (KBr): 3055, 2960, 2870, 2212, 1588, 1515, 1445, 1162, 895, 763,646cm^{-1}

HRMS (ESI): *m/z* calculated for $C_{34}H_{23}N_3Na$ $[M+Na]^+$: 496.1782; found; 496.1784.

2,16-Dimethoxy 5,13-dicyano *N*-butyl aza[7]helicene (17):

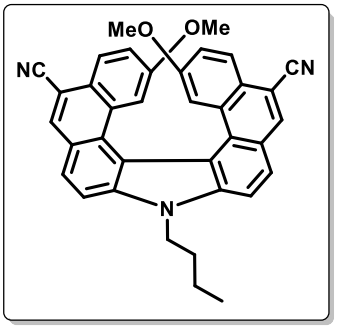

Yield = 71 %; Physical state = Yellow solid; m.p. = > 260 ^oC

^{1}H-NMR (400 MHz, $CDCl_3$):δ 8.44 (s, 2H), 8.17 (d, *J* = 8.8 Hz, 2H), 8.16 (d, *J* = 9.2 Hz, 2H), 8.07 (d, *J* = 8.8 Hz, 2H), 7.04 (dd, *J* = 8.8 and *J* = 2.4 Hz, 2H), 6.66 (d, *J* = 2.4 Hz, 2H), 4.82 (t, *J* = 7.2 Hz, 2H), 2.59 (s, 6H), 2.17-2.10 (m, 2H), 1.66-1.56 (m, 2H signal merged with water

peak), 1.08 (t, *J* = 7.2 Hz, 3H).

^{13}C-NMR (100 MHz, $CDCl_3$): δ 156.7, 141.0, 132.7, 131.1, 128.2, 127.8, 128.8, 125.4, 123.6, 119.2, 118.6, 116.1, 111.3, 107.5, 106.0, 53.8, 44.0, 32.1, 20.8, 14.0.

IR (KBr): 2957, 2925, 2680, 2213, 1586, 1516, 1444, 1339, 895, 797, 735 cm^{-1}

HRMS (ESI): *m/z* calculated for $C_{36}H_{27}N_3O_2Na$ $[M+Na]^+$: 556.1995; found; 556.1998.

2,5,13,16-Tetra cyano *N*-butyl aza[7]helicene(18):

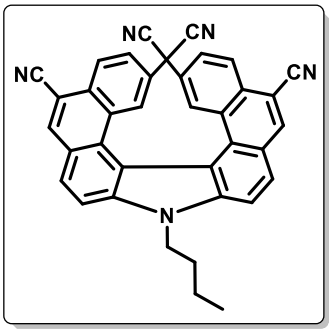

Yield = 67 %; Physical state = Yellow solid; m.p. = > 260 °C.

^{1}H-NMR (400 MHz, $CDCl_3$): δ 8.79 (s, 2H), 8.49 (d, *J* = 8.4 Hz, 2H), 8.36 (d, *J* = 8.8 Hz, 2H), 8.25 (d, *J* = 8.25 Hz, 2H), 7.62 (dd, *J* = 8.4 and *J* = 1.6 Hz, 2H), 7.44 (d, *J* = 1.2 Hz, 2H), 4.90 (t, *J* = 7.6 Hz, 2H), 2.19-2.12 (m, 2H),1.61(2H signal merged with water peak),1.08 (t, *J* = 7.6 Hz, 3H).

^{13}C-NMR (100 MHz, $CDCl_3$): Less signals due to poor solubility even after longer acquisition.

IR (KBr): 3047, 2876, 2819, 2226, 2209, 1630, 1581, 1487, 1413, 921, 839 cm^{-1}

HRMS (ESI): *m/z* calculated for $C_{36}H_{21}N_5Na$ $[M+Na]^+$: 546.1688; found; 546.1689.

***N*-(3-Phenyl propyl)-5,13-dicyano aza[7]helicene (19):**

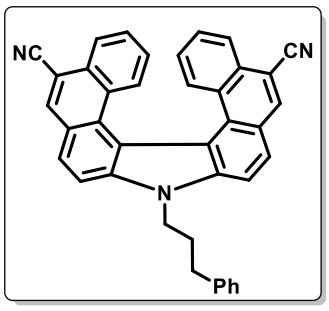

Yield = 83% Physical State = yellow solid m.p. :> 250 °C

^{1}H-NMR (400 MHz, $CDCl_3$): δ 8.54 (s, 2H), 8.25 (d, *J* = 8.0 Hz, 2H), 8.16 (d, *J* = 8.8 Hz, 2H), 7.92 (d, *J* = 8.8 Hz, 2H), 7.38-7.34 (m, 4H), 7.29-7.23 (m, 6H), 6.33-6.29 (m, 2H), 4.81 (t, *J* = 7.6 Hz, 2H), 2.91 (t, *J* = 7.6 Hz, 2H), 2.49 (quint, *J* = 6.8 Hz, 2H).

^{13}C-NMR (100 MHz, $CDCl_3$): δ 141.0, 140.2, 135.3, 129.3, 128.8, 128.7, 128.4, 128.3, 128.0, 127.9, 127.8, 126.5, 124.9, 124.2, 123.9, 118.5, 116.4, 110.7, 106.1, 43.2, 33.2, 30.7.

IR (KBr): 2957, 2922, 2212, 1577, 1518, 1465, 891, 822, 794 cm^{-1}

HRMS (APCI): *m/z* calculated for $C_{39}H_{25}N_3H$ $[M+H]^+$: 536.2117; found; 536.2121.

2,16-dicyano *N*-butyl aza[7]helicene (20):

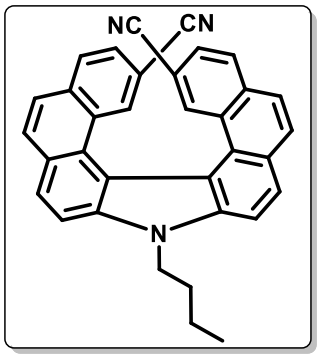

Yield = 27 %; Physical state = Yellow solid; m.p. = >260 ^{o}C

^{1}H-NMR (400 MHz, $CDCl_3$): δ 8.28 (d, *J* = 8.8 Hz, 2H), 8.25 (d, *J* = 8.4 Hz, 2H), 8.12 (d, *J* = 8.8 Hz, 2H), 8.04 (d, *J* = 8.0 Hz, 2H), 8.03 (d, *J* = 8.8 Hz, 2H), 7.50 (d, *J* = 1.2 Hz, 2H), 7.41 (dd, *J* = 8.0 and 1.6 Hz, 2H), 4.85 (t, *J* = 7.6 Hz, 2H), 2.19-2.08 (m, 2H), 1.59-1.55 (m, 2H signal merged with water peak), 1.06 (t, *J* = 7.2 Hz, 3H)

^{13}C-NMR (100 MHz, $CDCl_3$): δ 139.8, 133.6, 133.5, 130.6, 128.3, 128.0, 127.4, 127.2, 126.9, 125.3, 123.9, 118.4, 115.8, 111.1, 105.3, 43.7, 31.9, 20.7, 13.9.

IR (KBr): 2929, 2851, 2227, 1634, 1553, 1283, 1245, 1155, 907, 803, 749 cm^{-1}

HRMS (ESI): *m/z* calculated for $C_{34}H_{23}N_3Na$ $[M+Na]^+$: 496.1784; found; 496.1789.

(9-Butyl-9*H*-carbazole-3,6-diyl)dimethanol (24):

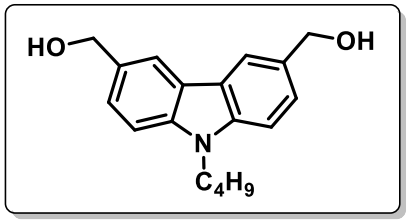

3,6-diformyl-9-butyl-9*H*-carbazole (2.0 g, 7.2 mmol) was dissolved in MeOH/CH_2Cl_2 (15 mL each). $NaBH_4$ (0.53 g, 14.33 mmol) was then added and stirred for 0.5 h at room temperature. The solvent was removed under reduced pressure and the crude product was purified by column chromatography on silica gel using petroleum ether–ethyl acetate (50:50) as eluent to afford (9-butyl-9*H*-carbazole-3,6-diyl)dimethanol **24**.

^{1}H-NMR (400 MHz, $CDCl_3$): δ 8.10 (d, *J* = 0.8 Hz, 2H), 7.50 (dd, *J* = 8.4 and 1.6 Hz, 2H), 7.41 (d, *J* = 8.4 Hz, 2H), 4.86 (s, 4H), 4.32 (t, *J* = 7.2 Hz, 2H), 1.89-1.82 (m, 2H), 1.43-1.34 (m, 2H), 0.95 (t, *J* = 7.6 Hz, 3H).

2-(4-Methoxyphenyl)-3-phenylacrylonitrile (29):

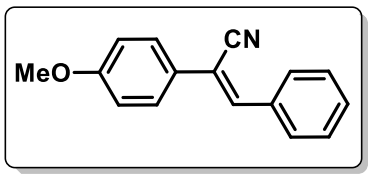

A mixture of *p*-benzyl cyanide **27** (3.0 g; 20.7 mmol), finely ground solid KOH (2.1 g; 37.6 mmol) and benzaldehyde **28** (2.0 g; 18.8 mmol) in methanol (30 mL) was stirred at room temperature for 6 hours. The resultant reaction mixture was concentrated under reduced pressure, poured into water

and extracted using ethyl acetate (3X50 mL). The combined organic layer was dried over sodium sulfate and concentrated to give crude **29** as pale yellow solid (4.5 g, 94%); which is recrystallized from ethyl acetate-petroleum ether to get white solid.

^{1}H-NMR (400 MHz, $CDCl_3$): δ 7.89 (dd, *J* = 7.2 and 1.6 Hz, 2H), 7.65-7.62 (m, 2H), 7.50-7.41 (m, 4H), 7.50-7.41 (m, 4H), 7.0-6.96 (m, 2H), 3.87 (s, 3H)

3-Methoxyphenanthrene-9-carbonitrile (30):

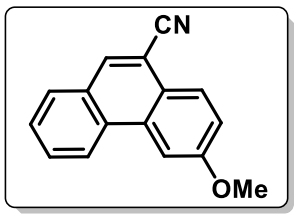

A solution of **29** (1.0 g, 4.25 mmol) and iodine (1.18 g, 4.68 mmol) in toluene (1250 mL) and tetrahydrofuran (17.0 mL, 210.3 mmol, 50 equivalent) was irradiated in a standard immersion well photoreactor with 250W high pressure mercury vapor lamp for 48 hours. The reaction mixture was then washed with aqueous sodium thiosulfate and dried over anhydrous sodium sulfate. The concentrated mixture was purified on silica gel column using ethyl acetate and petroleum ether (1:4) to afford **30** as pale yellow solid (0.93 g, 94%)

^{1}H-NMR (400 MHz, $CDCl_3$): δ 8.62 (d, *J* = 8.4 Hz, 1H), 8.22 (d, *J* = 8.8 Hz, 1H), 8.12 (s, 1H), 8.06 (d, *J* = 2.8 Hz, 1H), 7.94-7.92 (m, 1H), 7.81-7.77 (m, 1H), 7.71-7.67 (m, 1H), 7.39 (dd, *J* = 8.8 and 2.4 Hz, 1H), 4.06 (s, 3H)

3-Hydroxyphenanthrene-9-carbonitrile (31):

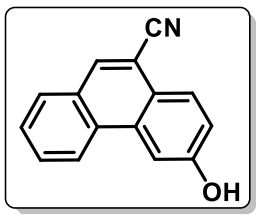

To a round bottom flask, was added **30** (1.0 g, 4.29 mmol) and anhydrous aluminium chloride $AlCl_3$ (1.14 g, 8.58 mmol) in dimethyl formamide (50 mL, followed by heating in an oil bath to 180^{o}C for 24 hours. The reaction mixture was then allowed to cool to room. Water was added to the reaction mixture and it was allowed to stir till solution becomes clear. It was extracted using ethyl acetate (3X50 mL). The combined organic layer was dried over sodium sulfate and concentrated under reduced pressure. The concentrated mixture was purified on silica gel column using ethyl acetate and petroleum ether (2:3) to afford **31** as pale yellow solid (0.53 g, 56%).

^{1}H-NMR (400 MHz, $CDCl_3$): δ 8.57 (d, *J* = 8.0 Hz, 1H), 8.22 (d, *J* = 8.8 Hz, 1H), 8.14 (s, 1H), m8.09 (d, *J* = 2.0 Hz, 1H), 7.94 (d, *J* = 8.0 Hz, 1H), 7.81-7.77 (m, 1H), 7.71-7.67 (m, 1H), 7.32 (dd, *J* = 8.8 and 2.4 Hz, 1H), 5.46 (s, 1H)

3,3'-Dihydroxy-[4, 4'-biphenanthrene]-9,9'-dicarbonitrile (32):

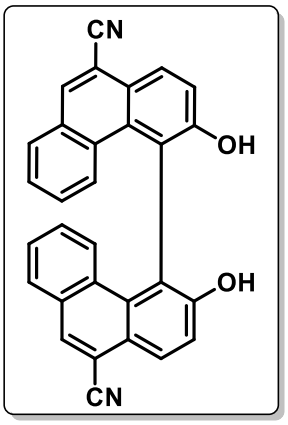

In a 50mL round bottom flask, a mixture of 3-hydroxyphenanthrene-9-carbonitrile **31** (0.2 g, 0.9 mmol), $CuCl(OH)[(Me_2N)_2CH_2CH_2(NMe_2)_2]$ (0.21 g, 0.9 mmol) in methanol (25 mL) was placed and was sonicated for 10 mins. The reaction mixture was stirred at room temperature. The reaction mixture was concentrated to remove methanol and 1 *M* aqueous HCl was added. The resulting mixture was extracted with ethyl acetate (3X50 mL). The organic layer was dried over anhydrous Na_2SO_4, filtered, and concentrated under reduced pressure. Purification of the crude residue by silica gel column chromatography with petroleum ether/ethyl acetate (1:1) as an eluent gave the **32** as a colorless solid (0.145 g, 73%)

^{1}H NMR (400 MHz, DMSO-*d6*): δ 9.79 (s, 2H), 8.49 (s, 2H), 8.25 (d, *J* = 8.8 Hz, 2H), 8.04-8.0 (m, 4H), 7.53 (d, *J* = 8.8 Hz, 2H), 7.47 (t, *J* = 7.2 Hz, 2H), 7.12-7.08 (m, 2H).

3,3'-Dinonaflate-[4,4'-biphenanthrene]-9,9'-dicarbonitrile (33):

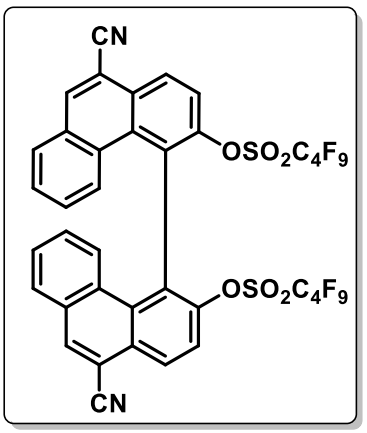

A mixture of **32** (0.1 g, 0.23 mmol) and triethylamine (0.16 mL, 1.15 mmol) in dimethyl formamide (25 mL) was placed in a round bottom flask. To this solution was slowly added nonafluorobutanesulfonyl fluoride (0.103 mL, 0.57 mmol) at 0 °C. The reaction mixture was stirred at 70 °C for 8 hours. The resultant reaction mixture was poured into water and extracted using ethyl acetate (3X50 mL). The combined organic layer was dried over sodium sulfate. Purification of the crude residue by silica gel column chromatography with petroleum ether/ethyl acetate (90:10) as an eluent gave **33** as a white solid (0.158 g, 69%).

^{1}H-NMR (400 MHz, $CDCl_3$): δ 8.72 (d, *J* = 9.2 Hz, 2H), 8.49 (s, 2H), 8.02 (d, *J* = 7.6 Hz, 2H), 7.89-7.84 (m, 4H), 7.63 (t, *J* = 7.2 Hz, 2H), 7.26-7.21 (m, 2H).

4.13 Spectral data:

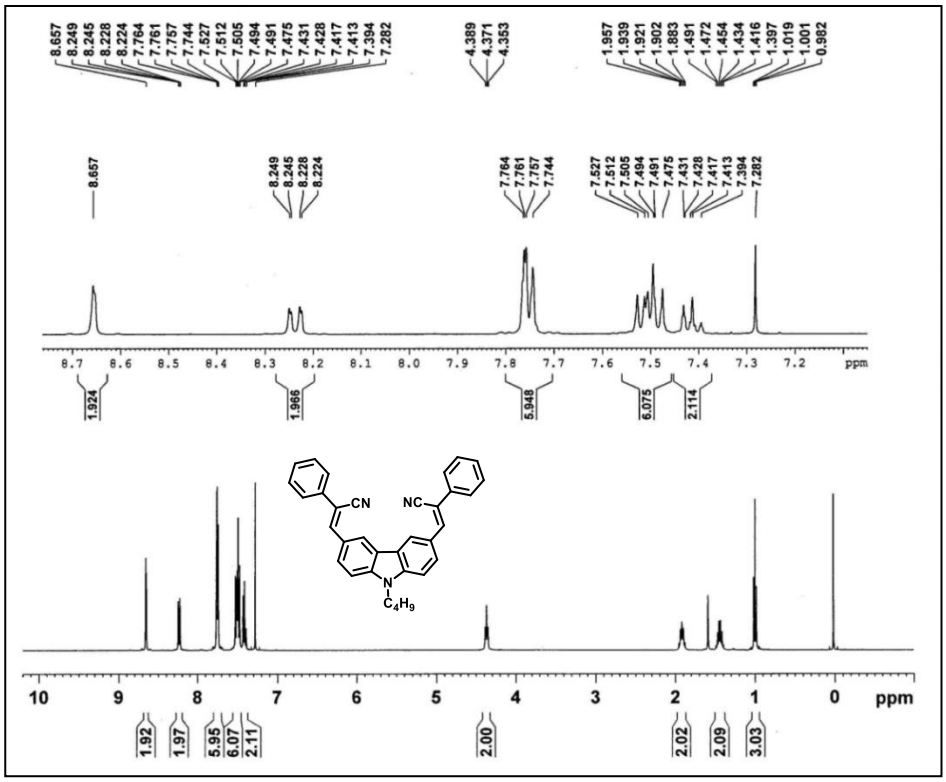

^{1}H-NMR of compound 15 ($CDCl_3$, 400 MHz)

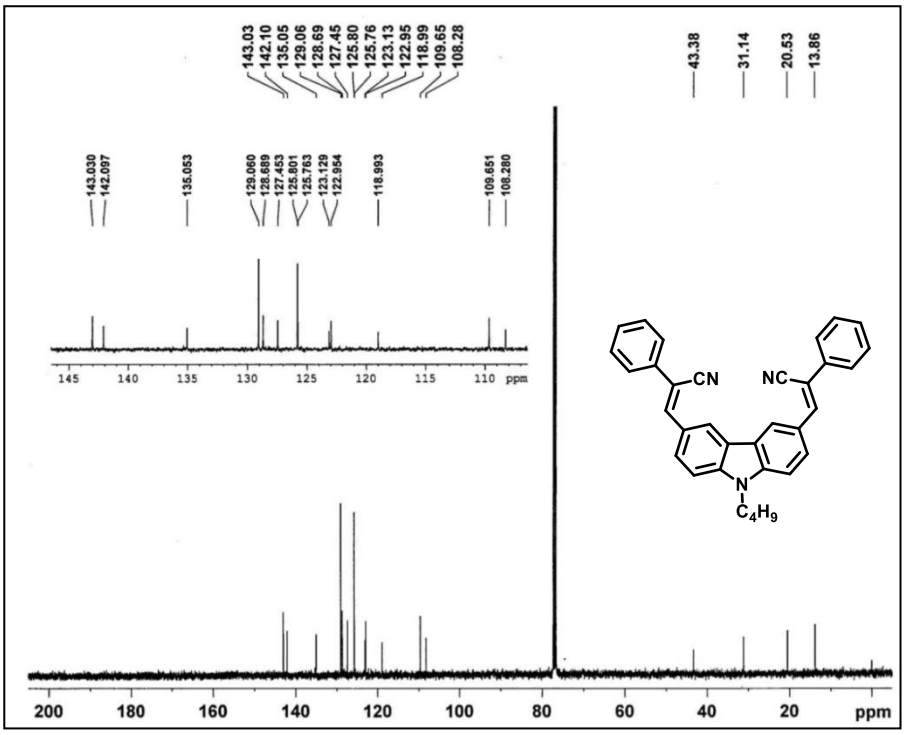

^{13}C-NMR of compound 15 ($CDCl_3$, 100 MHz)

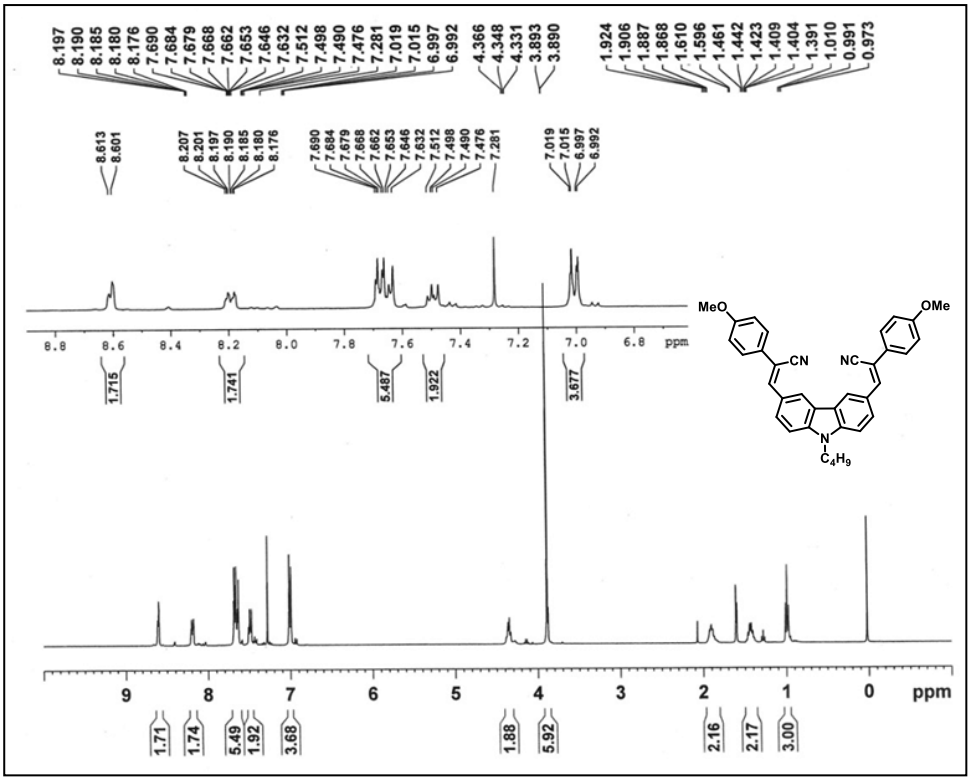

^{1}H-NMR of compound 15a ($CDCl_3$, 400 MHz)

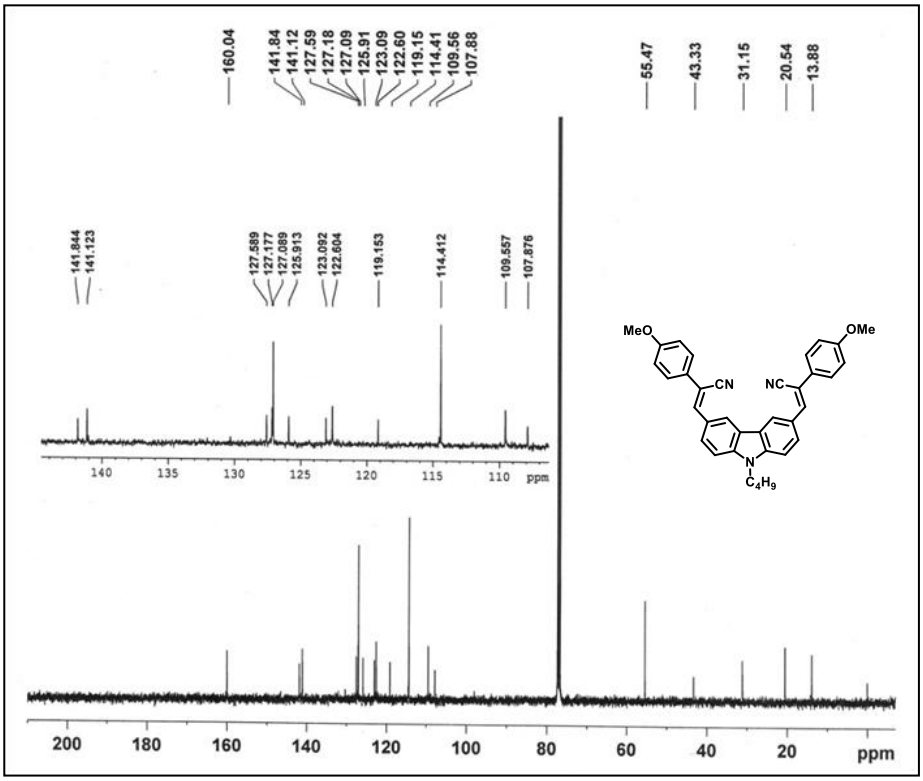

^{13}C-NMR of compound 15a ($CDCl_3$, 100 MHz)

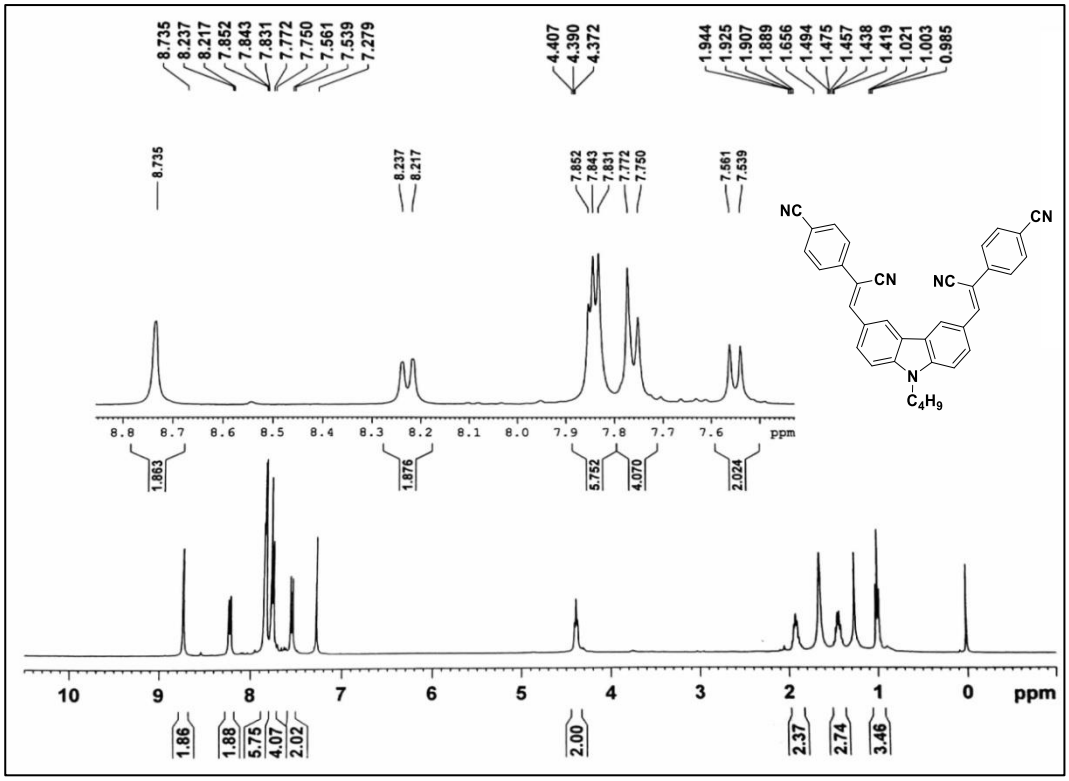

^{1}H-NMR of compound 15b ($CDCl_3$, 400 MHz)

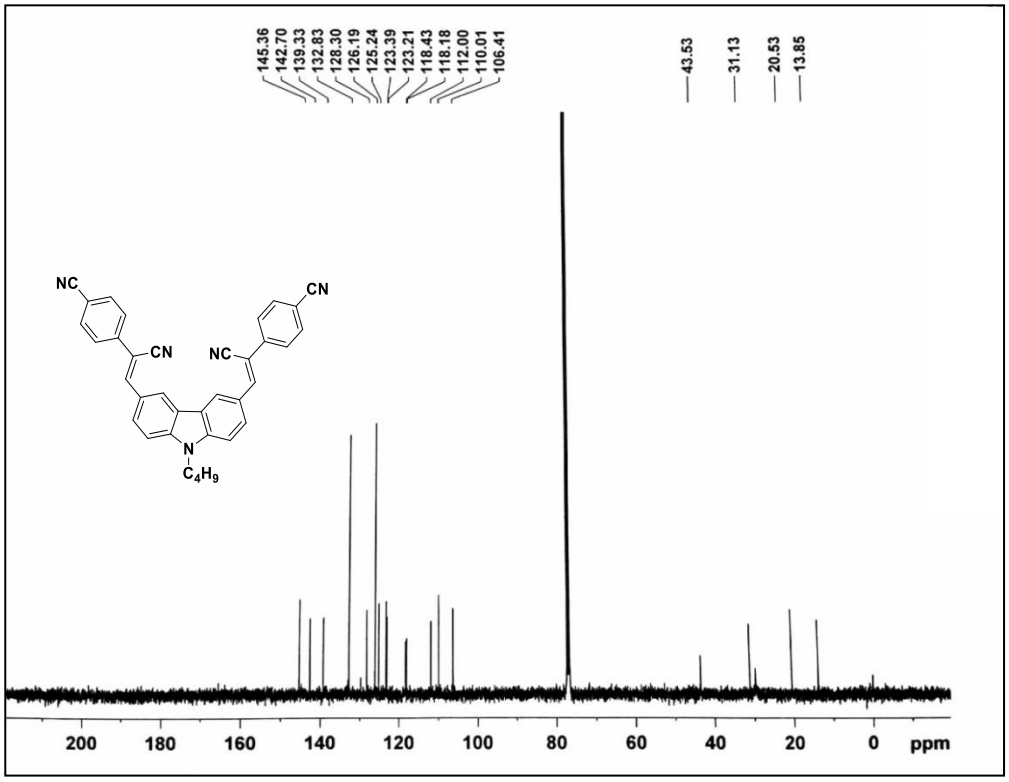

^{13}C-NMR of compound 15b ($CDCl_3$, 100 MHz)

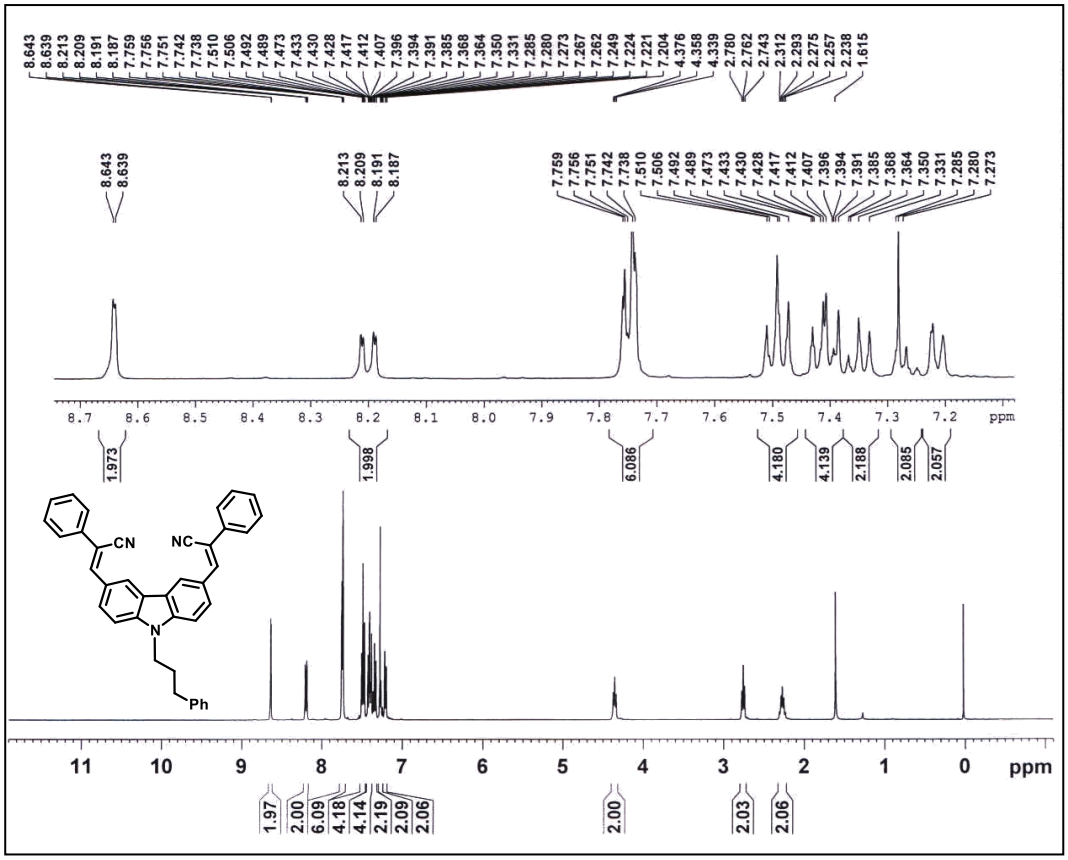

^{1}H-NMR of compound 15c ($CDCl_3$, 400 MHz)

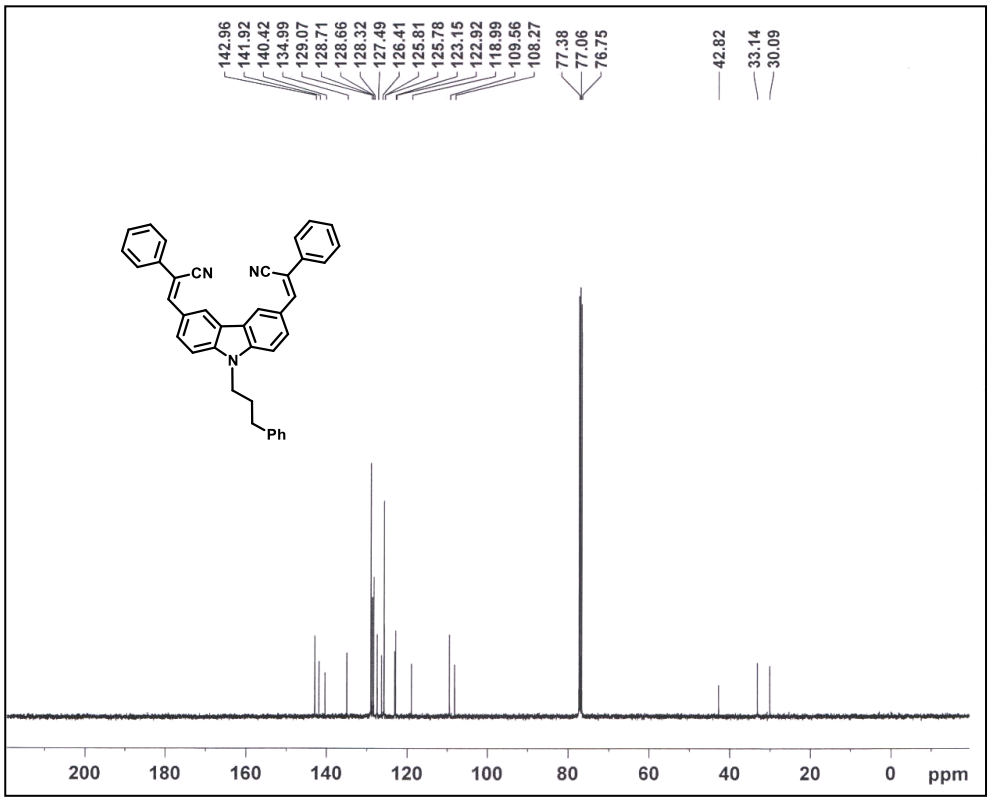

^{13}C-NMR of compound 15c ($CDCl_3$, 100 MHz)

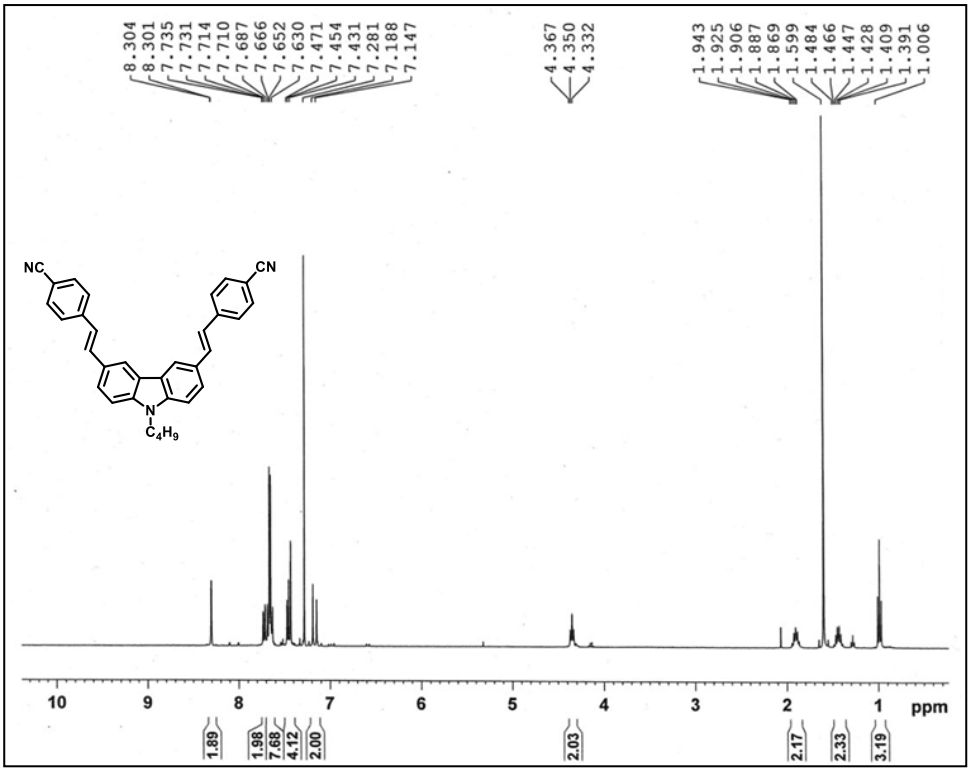

^{1}H-NMR of compound 15d ($CDCl_3$, 400 MHz)

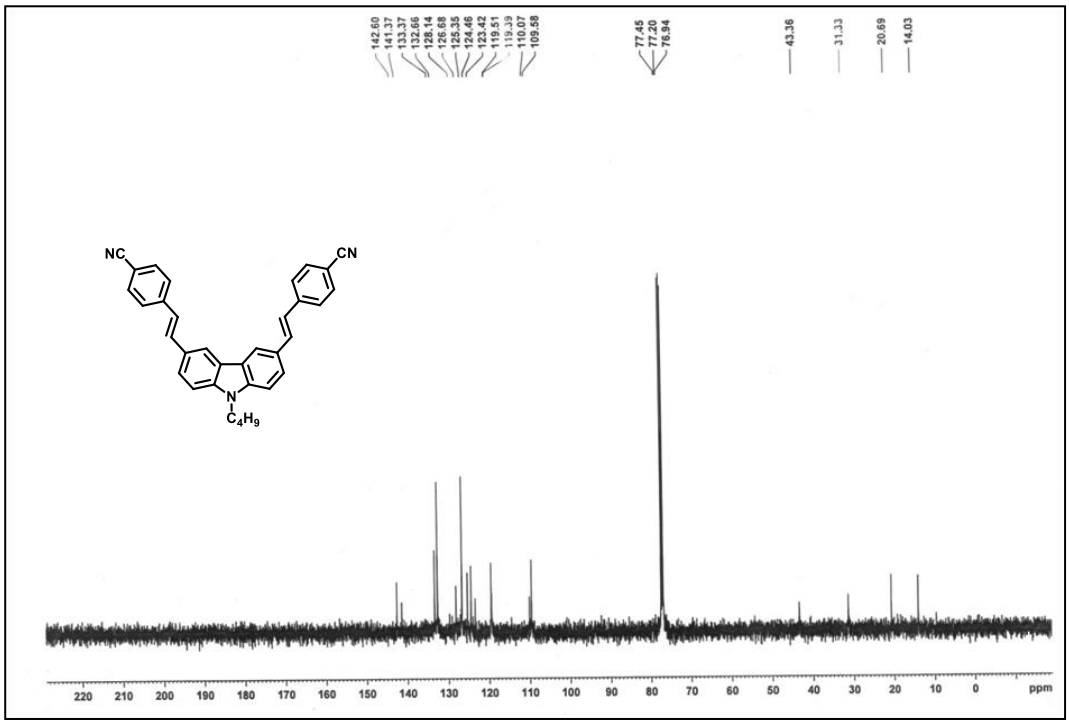

^{13}C-NMR of compound 15d ($CDCl_3$, 100 MHz)

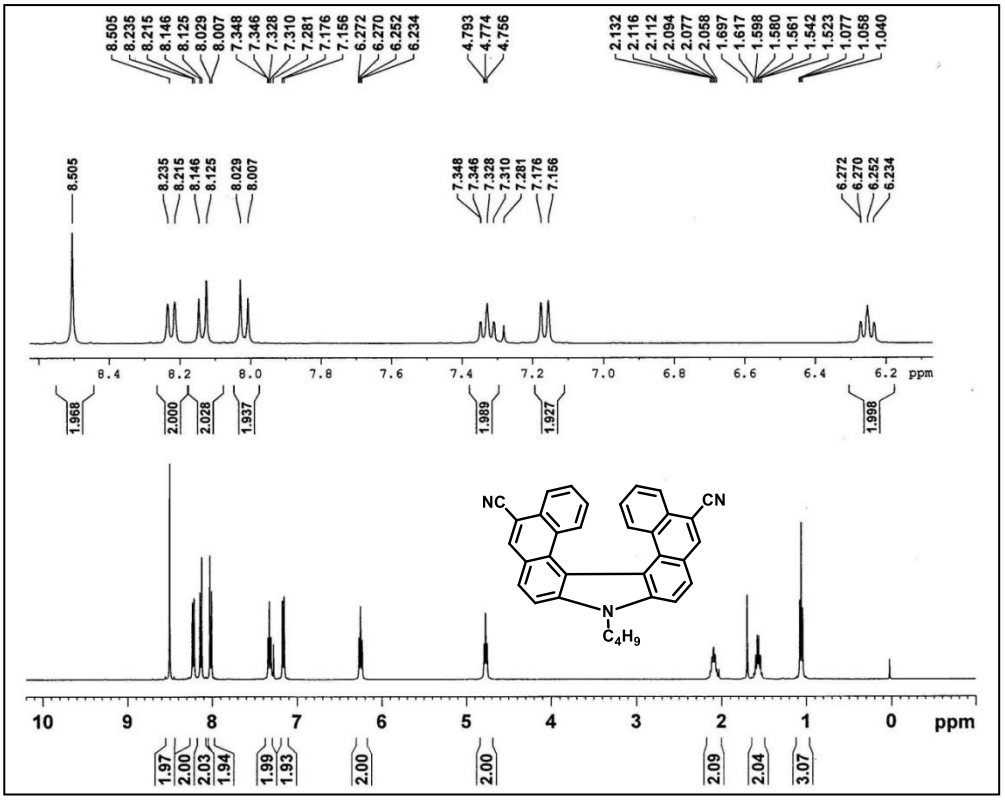

^{1}H-NMR of compound 16 ($CDCl_3$, 400 MHz)

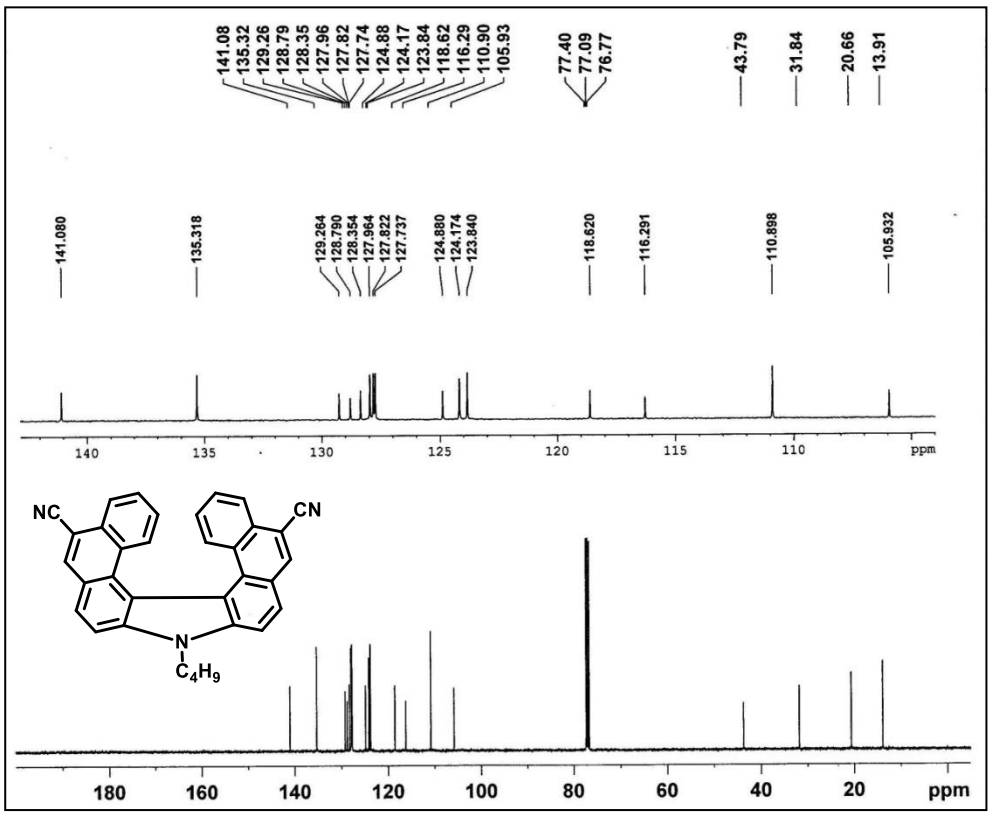

^{13}C-NMR of compound 16 ($CDCl_3$, 100 MHz)

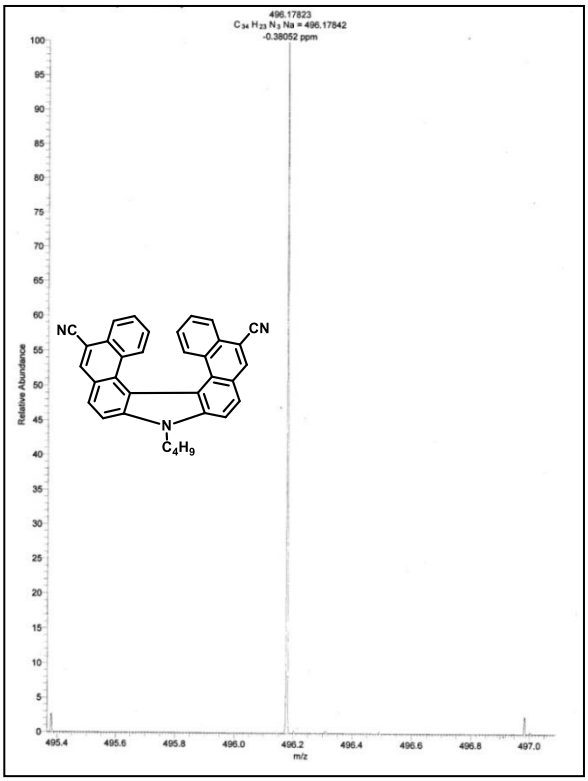

HRMS of compound 16

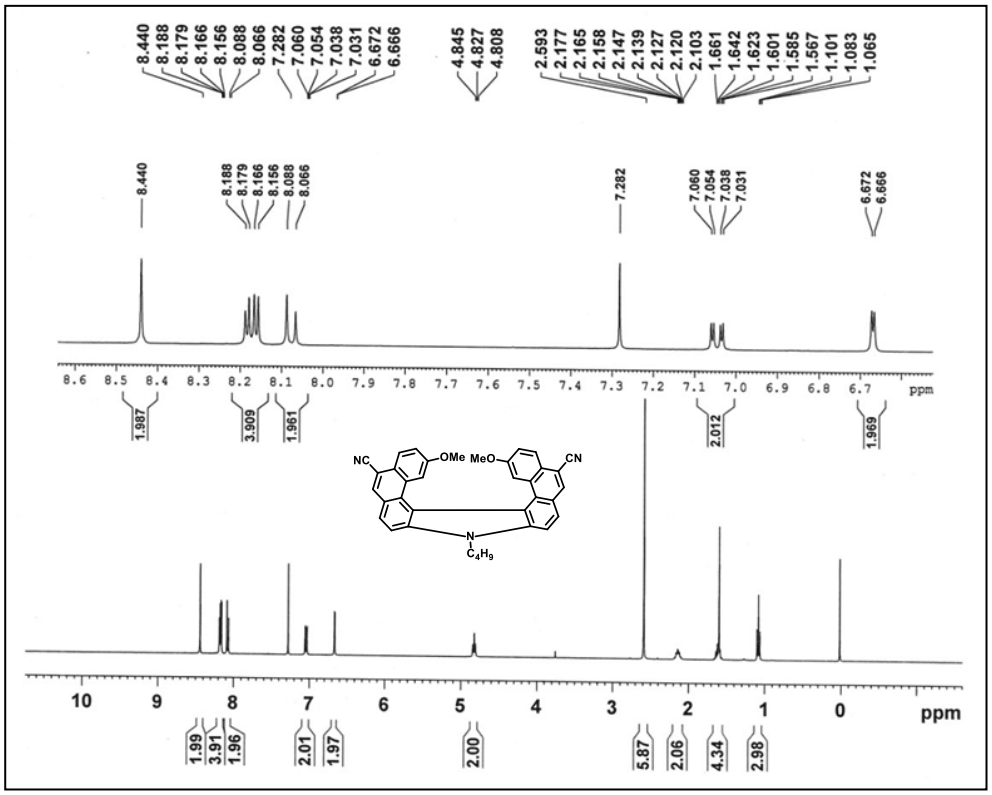

^{1}H-NMR of compound 17 ($CDCl_3$, 400 MHz)

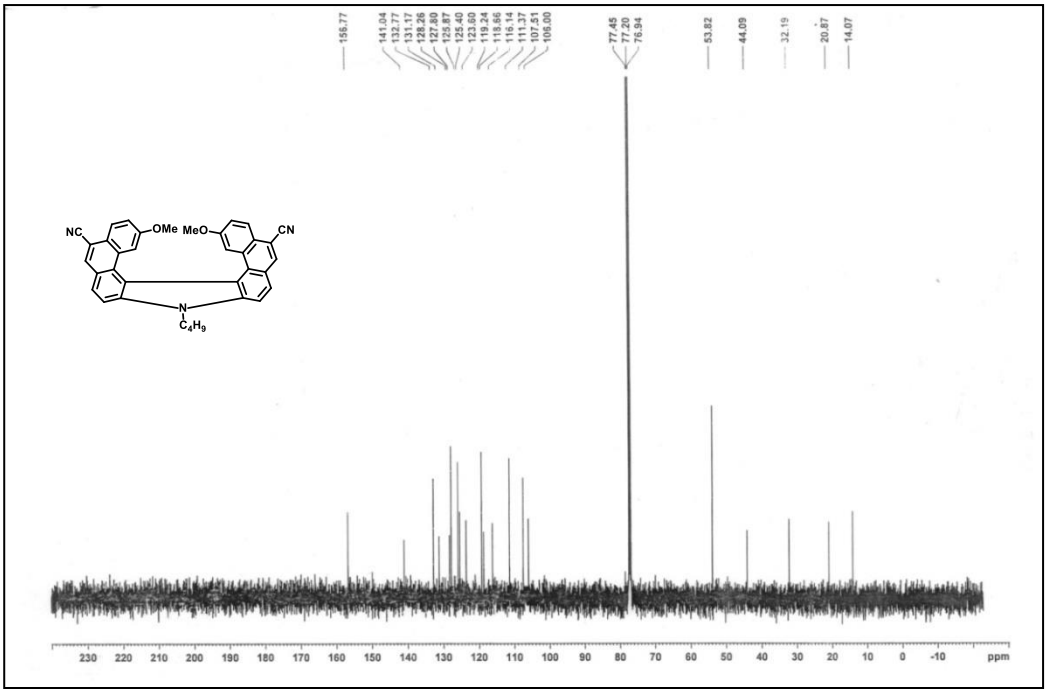

^{13}C-NMR of compound 17($CDCl_3$, 100 MHz)

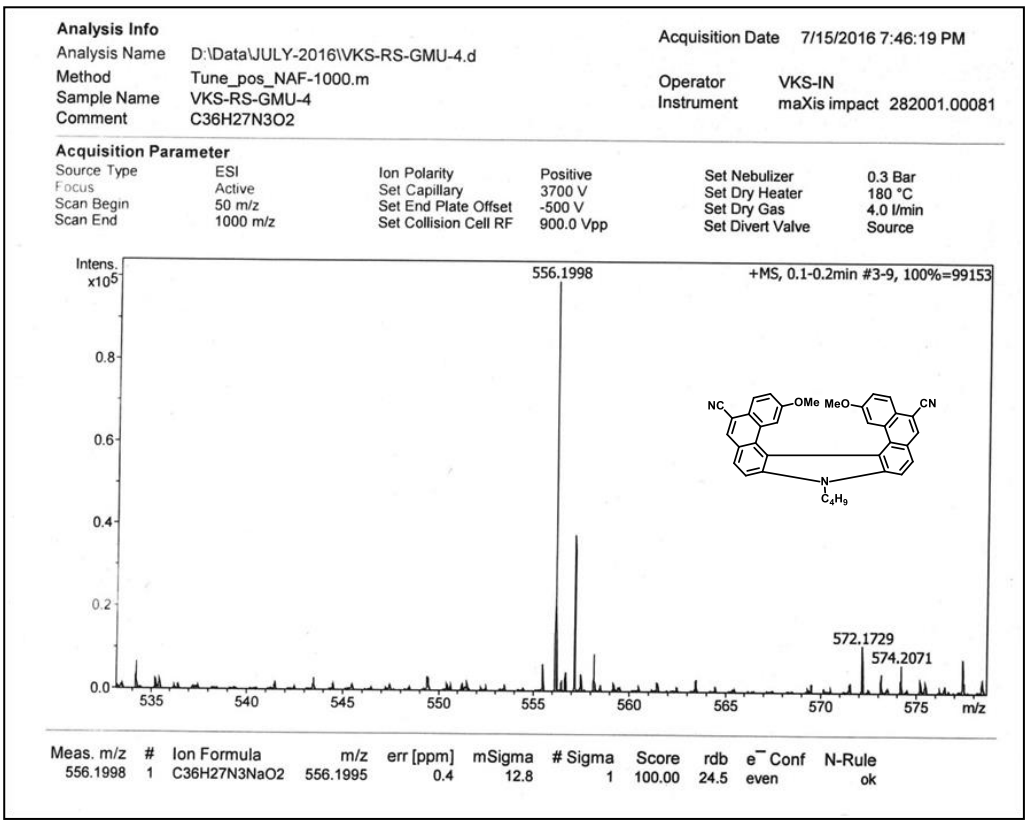

HRMS of compound 17

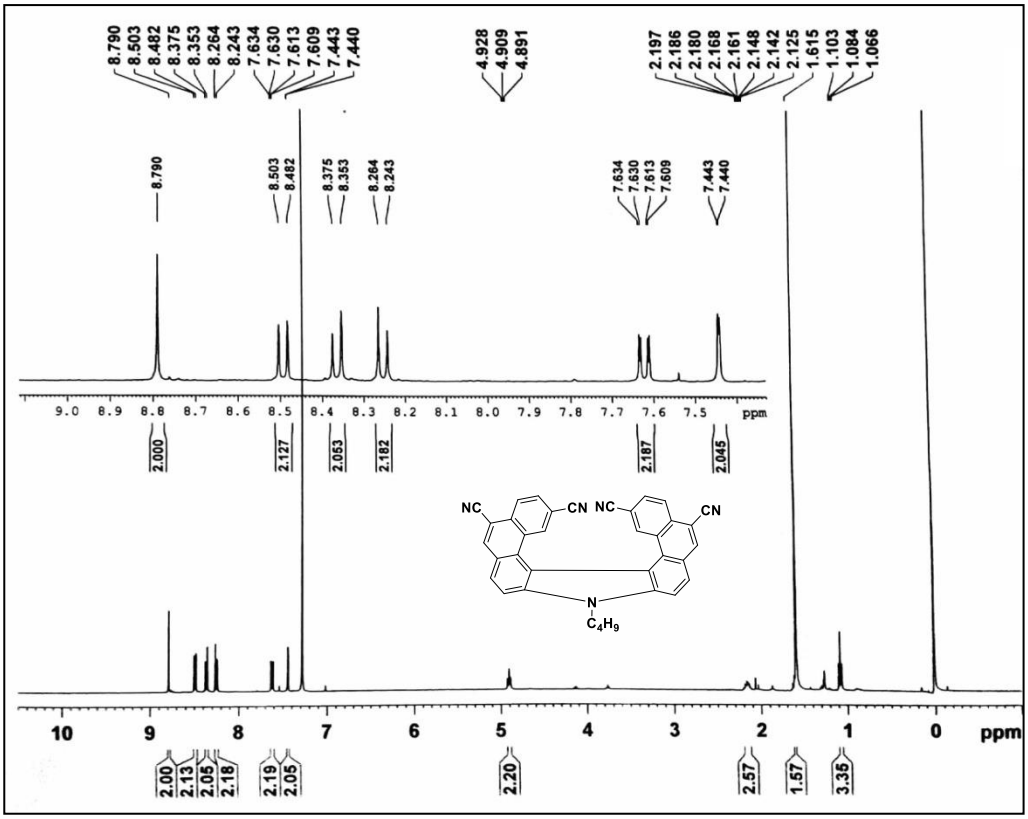

^{1}H-NMR of compound 18 ($CDCl_3$, 400 MHz)

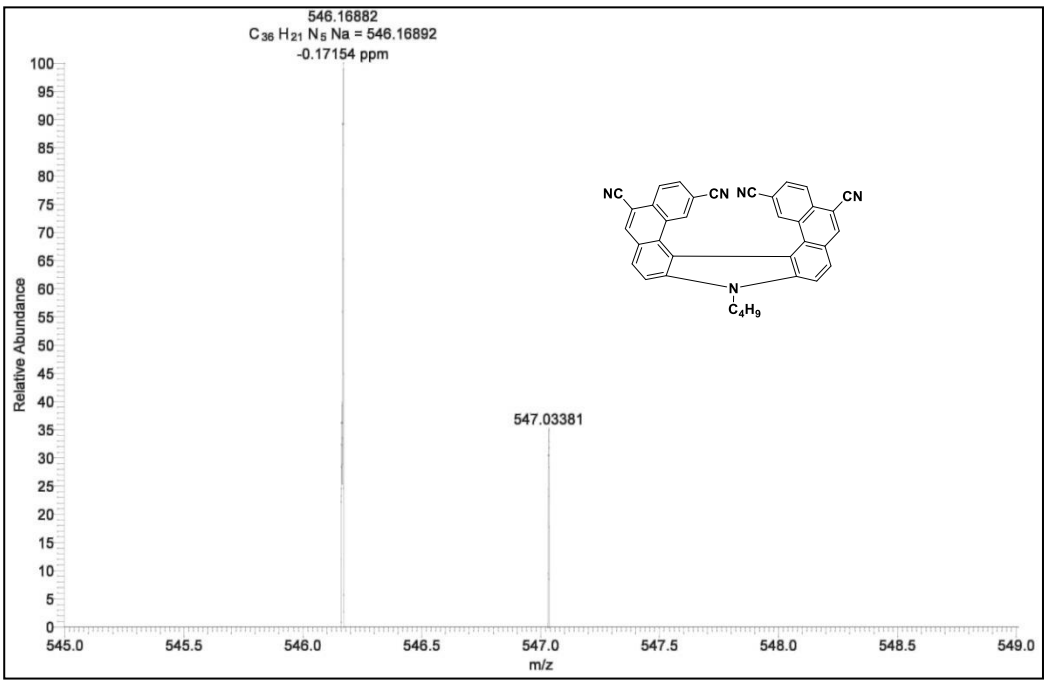

HRMS of compound 18

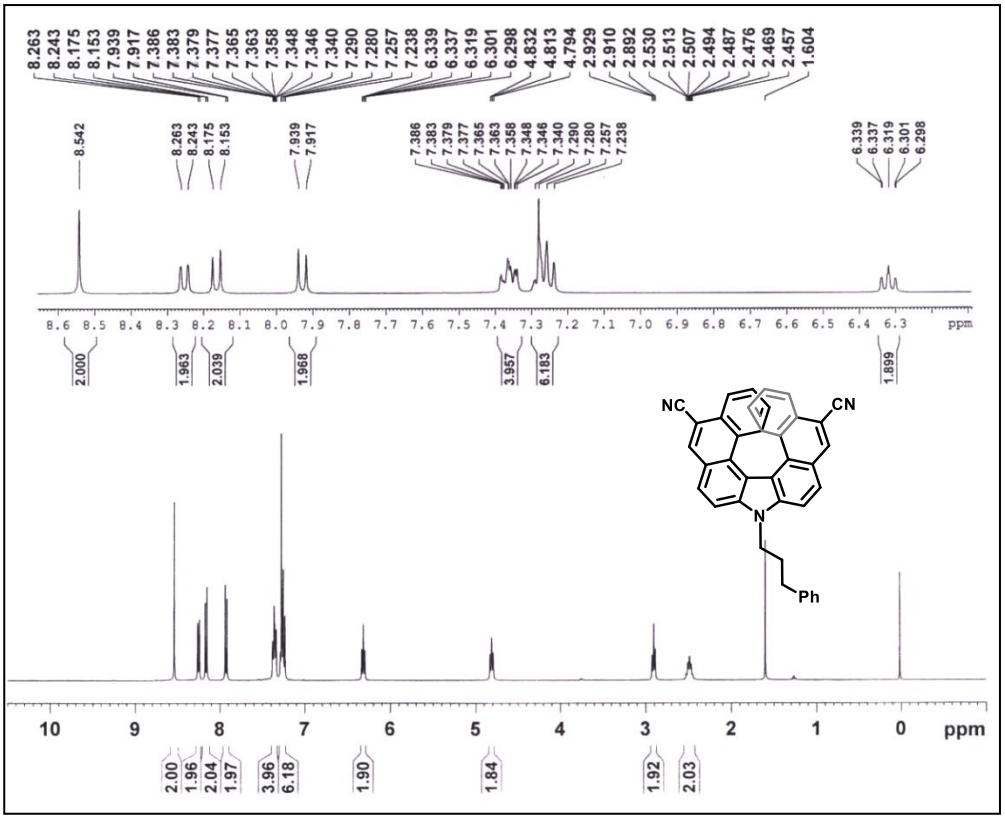

^{1}H-NMR of compound 19 ($CDCl_3$, 400 MHz)

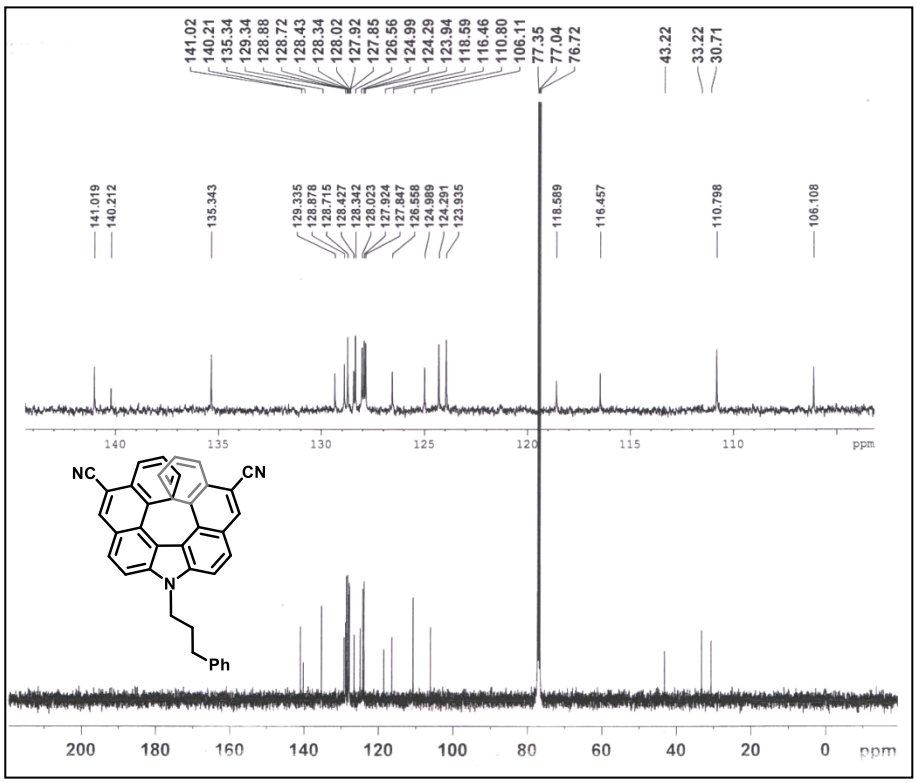

^{13}C-NMR of compound 19 ($CDCl_3$, 100 MHz)

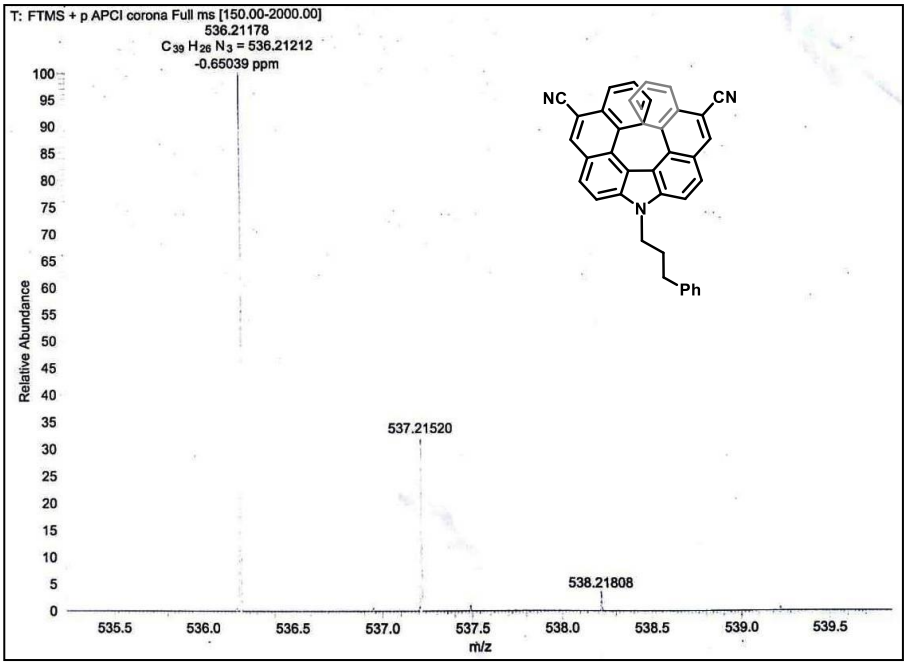

HRMS of compound 19

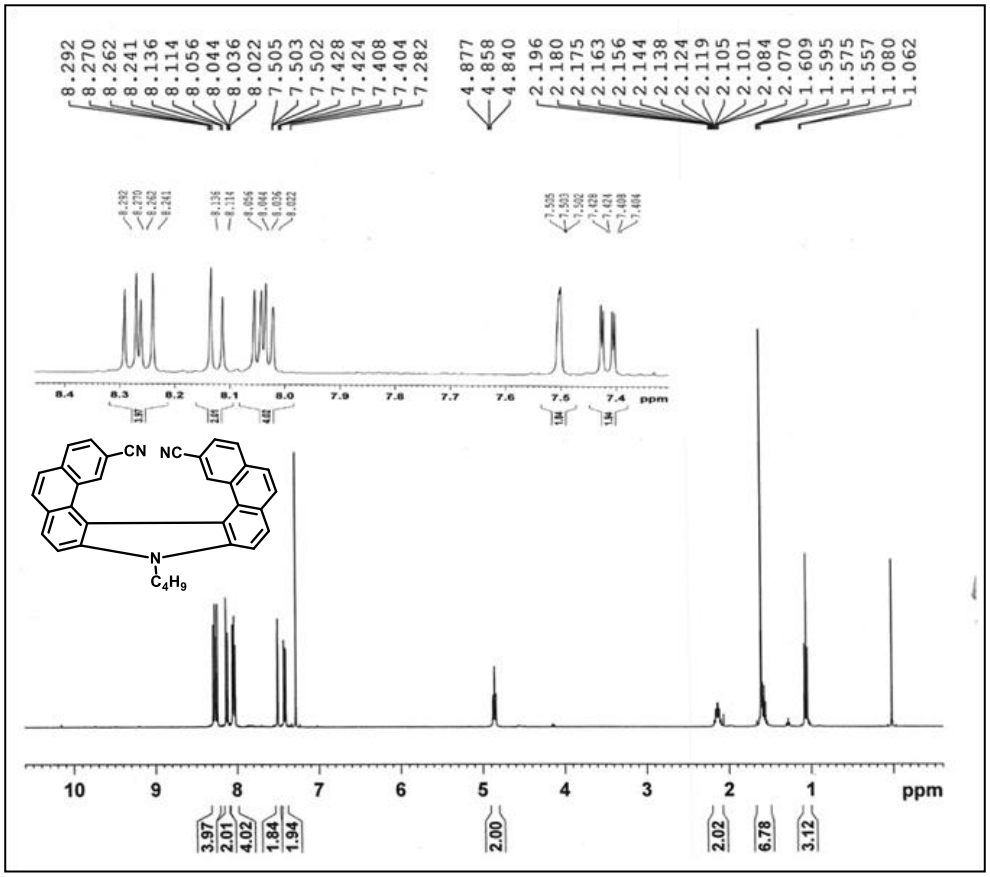

^{1}H-NMR of compound 20 ($CDCl_3$, 400 MHz)

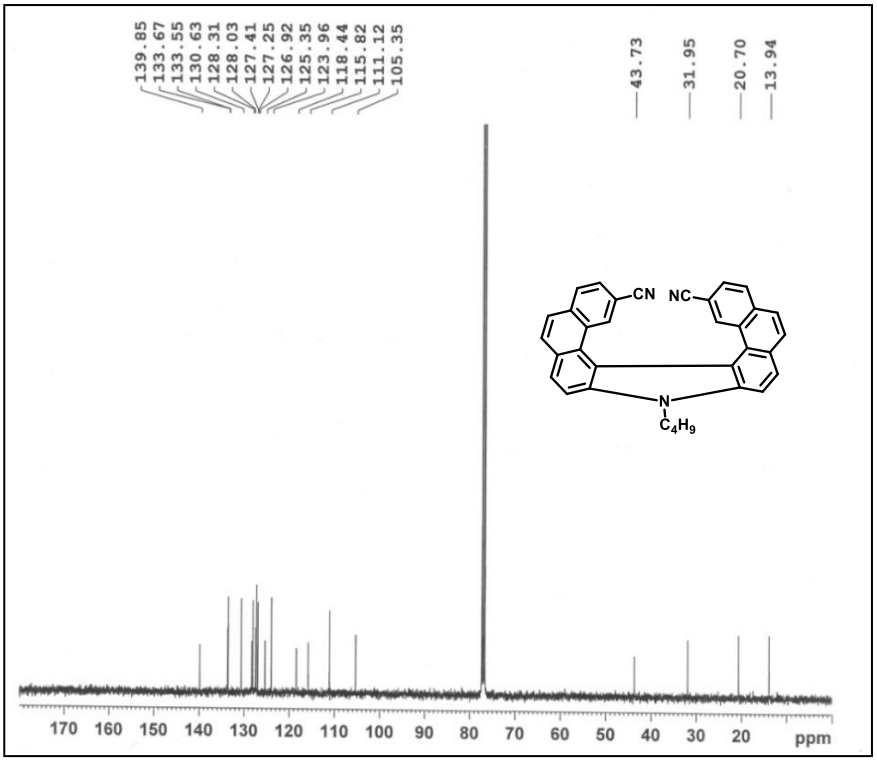

^{13}C-NMR of compound 20 ($CDCl_3$, 100 MHz)

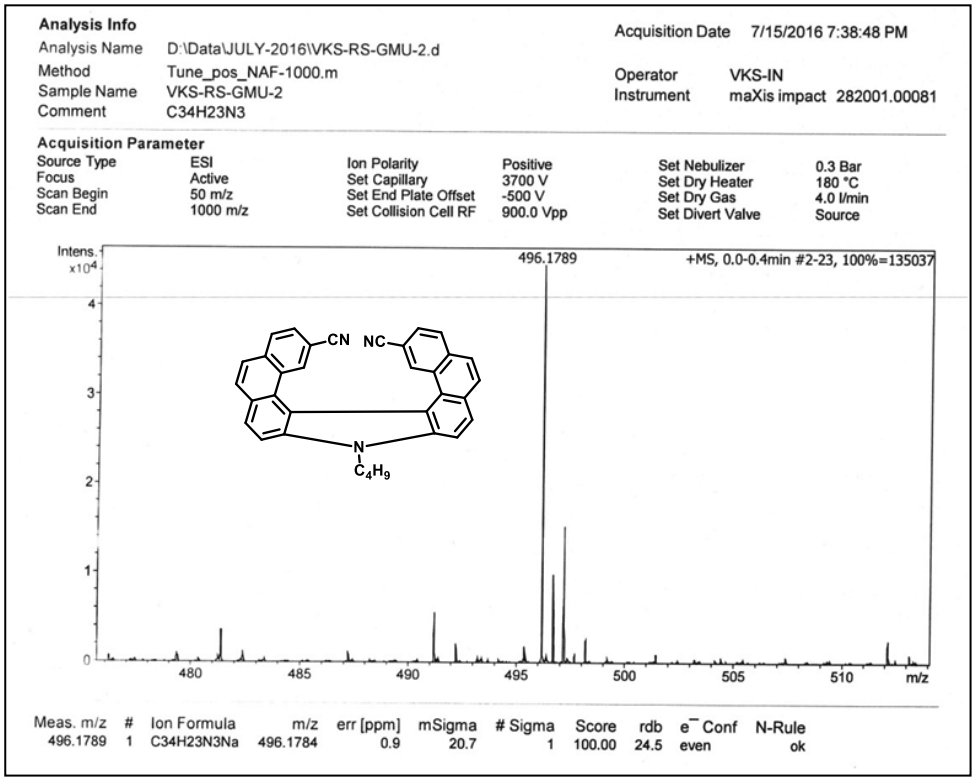

HRMS of compound 20

HPLC Chromatogram:

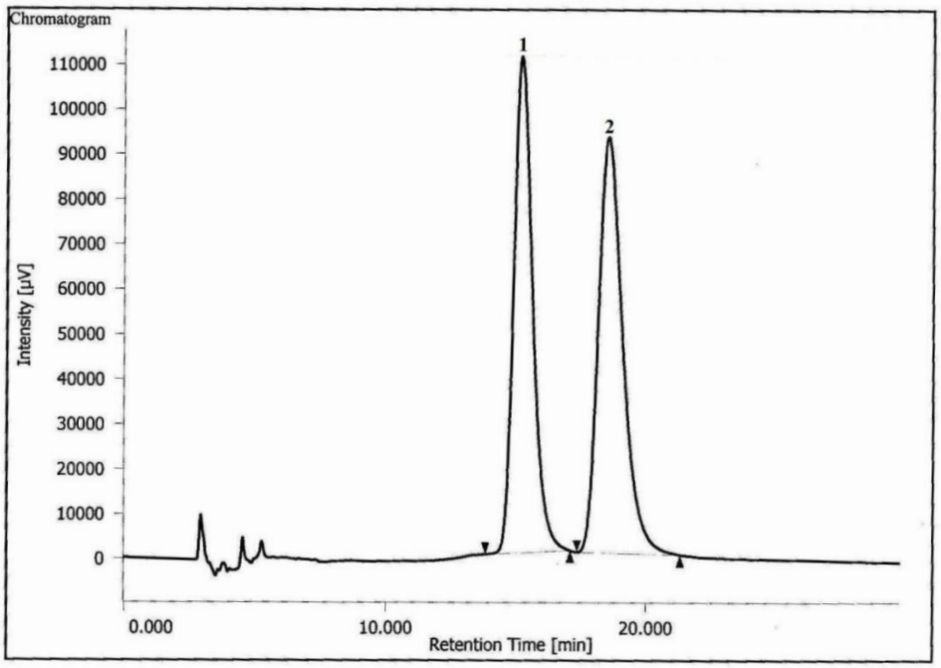

Peak Information

#	Peak Name	CH	tR [min]	Area [μV·sec]	Height [μV]	Area%	Height%	Quantity	NTP	Resolution	Symmetry Factor	Warning
1	Unknown	1	15.200	5551872	110391	47.892	54.422	N/A	2206	2.242	1.337	
2	Unknown	1	18.525	6040720	92453	52.108	45.578	N/A	1947	N/A	1.402	

HPLC chromatogram of racemic aza[7]helicene 16

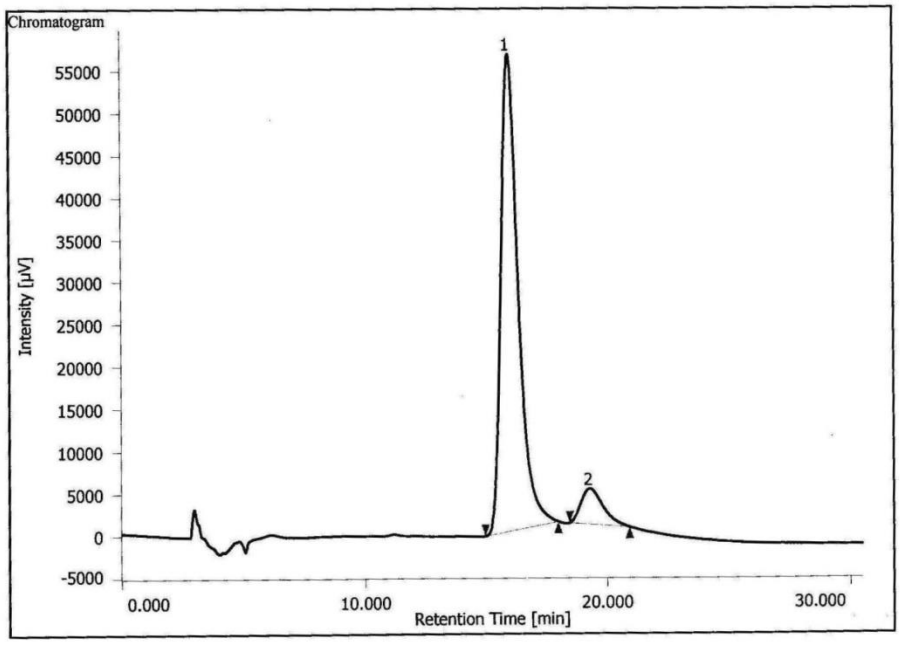

Peak Information

#	Peak Name	CH	tR [min]	Area [μV·sec]	Height [μV]	Area%	Height%	Quantity	NTP	Resolution	Symmetry Factor	Warning
1	Unknown	1	15.958	2794756	56460	91.354	93.065	N/A	2615	2.325	1.427	
2	Unknown	1	19.317	264499	4207	8.646	6.935	N/A	2197	N/A	1.369	

HPLC chromatogram of *P* aza[7]helicene 16 (ee = 82.71%)

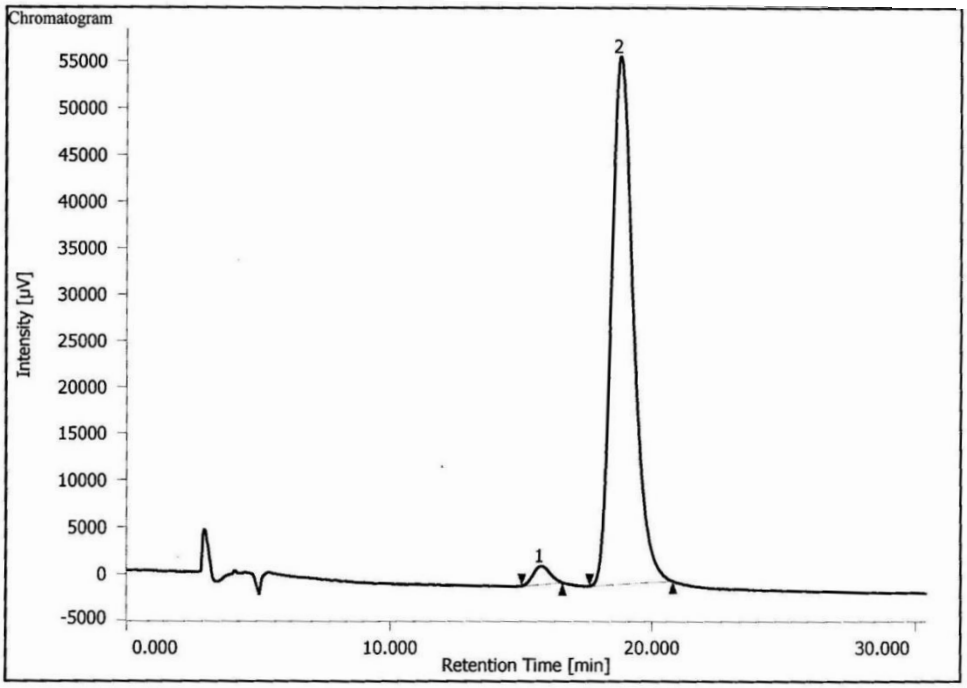

Peak Information

#	Peak Name	CH	tR [min]	Area [µV·sec]	Height [µV]	Area%	Height%	Quantity	NTP	Resolution	Symmetry Factor	Warning
1	Unknown	1	15.783	88055	1972	2.593	3.364	N/A	2685	2.204	1.074	
2	Unknown	1	18.783	3308449	56652	97.407	96.636	N/A	2473	N/A	1.316	

HPLC chromatogram of *M* aza[7]helicene 16 (ee =94.81%)

HPLC Conditions: Chiral column: Chiralcel OD-H, Solvent system (80:20, n-hexane: isopropanol, UV-254 nm), Flow rate = 1.0 mL/min.

4.14 References:

1. Grimme, S. *Angew. Chem. Int. Ed.* **2008**, *47*, 3430.
2. Cerný, J.; M. Kabelác, M.; P. Hobza, P. *J. Am. Chem. Soc.* **2008**, *130*, 16055.
3. (a) Flack, H.D. *Acta Cryst*. **2009**, *A65*, 371. (b) Kostyanovsky, R. G. *Mandeleev Commun.* **2003**, *13*, 85.
4. Fumiao, T. Enatiomer Separation Fundamentals and Practical Methods, Springer-Verlag, Berlin, **2011**, 167-168.
5. (a) Pérez-García, L.; Amabilino, D. B. *Chem. Soc. Rev*. **2002**, *31*, 342. (b) Pérez-García, L.; Amabilino, D. B. *Chem. Soc. Rev*. **2007**, *36*, 941. (c) Jacques, J.; Collet, A.; Wilen, S.H. in *Enantiomers, racemates and resolution*, Malabar, F.L. (Ed.) Krieger Publishing Company, **1994**.
6. Gonnade, R. G.; Iwama, S.; Sugiwake, R.; Manoj, K.; Takahashi, H.; Tsue, H.; Tamura, R. *Chem. Commun.* **2012**, *48*, 2791.
7. Coquerel, G. Review on the heterogeneous equilibria between condensed phases in binary systems of enantiomers, *Enantiomer*, **2000**, Vol. 5, No. 5, 481-498, (Mai 2000), ISNN 1024-2430.
8. E. L. Eliel and S. H. Wilen, Stereochemistry of Organic Compounds, John Wiley & Sons, Inc., **1994**.
9. (a) Mooij, W. T. M.; Leusen, F. J. J. *Phys. Chem. Chem. Phys.*, **2001**, *3*, 5063. (b) Oria, D. E.; Karamertzanis, P. G.; Price, S. L. *Crystal Growth & Design*, **2010**, *10*, 1749.
10. McIntosh, A. O.; Robertson, J. M.; Vand, V. *Nature* **1952**, *169*, 322.
11. (a) Herbstein, F. H.; Schmidt, G. M. J. *J. Chem. Soc.* **1954**, 3302. (b) von Hahn, T. *Acta Crystallogr.* **1958**, *11*, 825. (c) Hirshfeld, F. L.; Sandler, S.; Schmidt, G. M. J. *J. Chem. Soc.* **1963**, 2108.
12. (a) Martin, R. H.; Flammang-Barbieux, M.; Cosyn, J. P.; Gelbcke, M. *Tetrahedron Lett.* **1968**, *30*, 3507. (b) Martin, R. H.; Flammang-Barbieux, M.; Cosyn, J. P.; Gelbcke, M. *ibid.* **1968**, 3507
13. Martin, R. H.; Marchant, M. J. *Tetrahedron* **1974**, *30*, 343.
14. Nuckolls, C.; Katz, T. J.; Castellanos, L. *J. Am. Chem. Soc.***1996**, *118*, 3767.
15. Phillips, K. E. S.; Katz, T. J.; Jockusch, S.; Lovinger, A. J.; Turro, N. J. *J. Am. Chem. Soc.* **2001**, *123*, 11899.
16. Nuckols, C.; Katz, T. J.; *J. Am. Chem. Soc.* **1998**, *120*, 9541.

17. Shcherbina, M. A.; Zeng, X. B.; Tadjiev, T.; Ungar, G.; Eichhorn, S. H.; Phillips, K. E. S.; Katz, T. J. *Angew. Chem. Int. Ed.* **2009**, *48*, 7837.
18. (a) Tanaka, K.; Shogase, Y.; Osuga, H.; Suzuki, H.; Nakanishi, W.; Nakamura, K.; Kawai, Y. *J. Chem. Soc.* **1995**, 1873. (b) Tanaka, K.; Kitahara, Y. *Chem. Commun.* **1998**, 1141. (c) Tanaka, K.; Kitahara, Y.; Suzuki, H.; Osuga, H.; Kawai, Y. *Tetrahedron Lett.* **1996**, *37*, 5925.
19. Murguly, E.; McDonald, R.; Branda, N. R. *Org. Lett*. **2000**, *2*, 3169.
20. Ernst, K. H.; Bohringer, M.; McFadden, C. F.; Hug, P.; Muller, U.; Ellerbeck, U. 1999. *Nanotechnology* **1999**, *10*, 355.
21. Taniguchi, M.; Nakagawa, H.; Yamagishi, A.; Yamada, K. *Surf. Sci*. **2000**, *454*, 1005.
22. Hauke, C. M.; Rahe, P.; Nimmrich, M.; Schütte, J.; Kittelmann, M.; Stará, I.G.; Starý, I. Rybáček, J.; Kühnle, A. *J. Phys. Chem. C* **2012**, *116*, 4637.
23. Parschau, M.; Fasel, R.; Ernst, K. H. *Cryst. Growth Des.* **2008**, *8*, 1890.
24. Seibel, J.; Allemann, O.; Siegel, J. S.; Ernst, K. H. *J. Am. Chem. Soc.* **2013**, *135*, 7434.
25. Balandina, T.; vander Meijden, M. W.; Ivasenko, O.; Cornil, D.; Cornil, J.; Lazzaroni, R.; Kellogg, R. M.; DeFeyter, S. *Chem. Commun.* **2013**, *49*, 2207.
26. Seibel, J.; Allemann, O.; Siegel, J. S.; Ernst, K. H. *J. Am. Chem. Soc.* **2013**, *135*, 7434.
27. (a) Fasel, R.; Parschau, M.; Ernst, K. H. *Nature* **2006**, *439*, 449; (b) Ernst, K. H.; Kuster, Y.; Fasel, R.; Müller, M.; Ellerbeck, U. *Chirality* **2001**, *13*, 675.
28. Fasel, R.; Cossy, A.; Ernst, K. H.; Baumberger, F.; Greber, T.; Osterwalder, J. *J. Chem. Phys.* **2001**, *115*, 1020.
29. (a) Ernst, K. H.; Neuber, M.; Grunze, M.; Ellerbeck, U. *J.* Am. *Chem. Soc.* **2001**, *123*, 493.
30. Ernst, K. H.; Böhringer, M.; McFadden, C. F.; Hug, P.; Müller, U.; Ellerbeck, U. *Nanotechnology*, **1999**, *10*, 355.
31. Kim, C.; Marks, T. J.; Facchetti, A.; Schiavo, M.; Bossi, A.; Maiorana, S.; Licandro, E.; Todescato, F.; Toffanin, S.; Muccini, M.; Graiff, C.; Tiripicchio, A. *Org. Electron*. **2009**, *10*, 1511.
32. Wachsmann, C.; Weber, E.; Czugler, M.; Seichter, W. *Eur. J. Org. chem*. **2003**, 2863.

33. (a) Stçhr, M.; Boz, S.; Schar M.; Nguyen, M. T.; Pignedoli, C. A.; Passerone, D.; Schweizer, W. B.; Thilgen, C.; Jung, T. A. Diederich, F.; *Angew. Chem. Int. Ed*. **2011**, *50*, 9982. (b) Shchyrba, A.; Nguyen, M. T.; Wackerlin, C.; Martens, S.; Nowakowska, S.; Ivas, T.; Roose, J.; Nijs, T.; Boz, S.; Schar, M.; Stohr, M.; Pignedoli, C. A.; Thilgen, C.; Diederich, F.; Passerone, D.; Jung, T. A. *J. Am. Chem. Soc.* **2013**, *135*, 15270.
34. Nakano, K.; Hidehira, Y.; Takahashi, K.; Hiyama, T.; Nozaki, K. *Angew. Chem. Int. Ed*. **2005**, *44*, 7136.
35. Miyasaka, M.; Rajca, A.; Pink, M.; Rajca, S. *Chem. Eur. J.* **2004**, *10*, 6531.
36. Kitahara, Y.; Tanaka, K. *Chem. Comm*. **2002**, 932.